PHYTOCHEMICAL ANALYSIS, BIOLOGICAL ACTIVITY, AND *IN SILICO* MOLECULAR DOCKING STUDIES OF CONSTITUENTS OF *SCADOXUS MULTIFLORUS* (MARTYN) RAF.

Ilili Dine

A Thesis Submitted to the Department of Applied Chemistry

School of Applied Natural Science

Presented in Partial Fulfillment of the Requirement for the Degree of Master's in Applied Chemistry (Natural Product Chemistry)

Office of Graduate Studies

Adama Science and Technology University

April 2023

Adama, Ethiopia

Phytochemical Analysis, Biological Activity and *In Silico* Molecular Docking Studies of Constituents of *Scadoxus multiflorus* (Martyn) Raf.

Ilili Dine

Advisor: Yadessa Melaku (Ph.D.)

Co-Advisor: Endale Mulugeta (Ph.D.)

A Thesis Submitted to the Department of Applied Chemistry

School of Applied Natural Science

Presented in Partial Fulfillment of the Requirement for the Degree of Master's in Applied Chemistry (Natural Product Chemistry)

Office of Graduate Studies

Adama Science and Technology University

April 2023

Adama, Ethiopia

DECLARATION

I hereby declare that this Master Thesis entitled "Phytochemical Analysis, Biological Activity and *in silico* Molecular Docking Studies of Constituents of *Scadoxus multiflorus* (Martyn) Raf" is my original work. That is, it has not been submitted for the award of any academic degree, diploma, or certificate in any other university. All sources of materials that are used for this thesis have been duly acknowledged through citation.

_____	_____	_____
Name of student	Signature	Date

RECOMMENDATION

We, the advisors of this thesis, hereby certify that we have read the revised version of the thesis entitled "Phytochemical Analysis, Biological Activity and *In silico* Molecular Docking Studies of Constituents of *Scadoxus multiflorus* (Martyn) Raf" prepared under our guidance by Ilili Dine submitted in partial fulfillment of the requirements for the degree of Masters of Science in Applied Chemistry (Natural Product Chemistry). Therefore, we recommend the submission of a revised version of the thesis to the department following the applicable procedures.

_____	_____	_____
Major Advisor	Signature	Date
_____	_____	_____
Co-advisor	Signature	Date

APPROVAL PAGE OF M.SC. THESIS

We, the advisors of the thesis entitled "Phytochemical Analysis, Biological Activity and *In Silico* Molecular Docking Studies of Constituents of *Scadoxus multiflorus* (Martyn) Raf" and developed by Ilili Dine, hereby certify that the recommendation and suggestions made by the board of examiners are appropriately incorporated into the final version of the thesis.

Major Advisor	Signature	Date
Co-advisor	Signature	Date

We, the undersigned, members of the Board of Examiners of the thesis by Ilili Dine have read and evaluated the thesis entitled Phytochemical Analysis, Biological Activity and *In Silico* Molecular Docking Studies of Constituents of *Scadoxus multiflorus* (Martyn) Raf" and examined the candidate during the open defense. This is, therefore, to certify that the thesis is accepted for partial fulfillment of the requirement of the degree of Master of Science in Applied Chemistry (Natural Product Chemistry).

Chairperson	Signature	Date

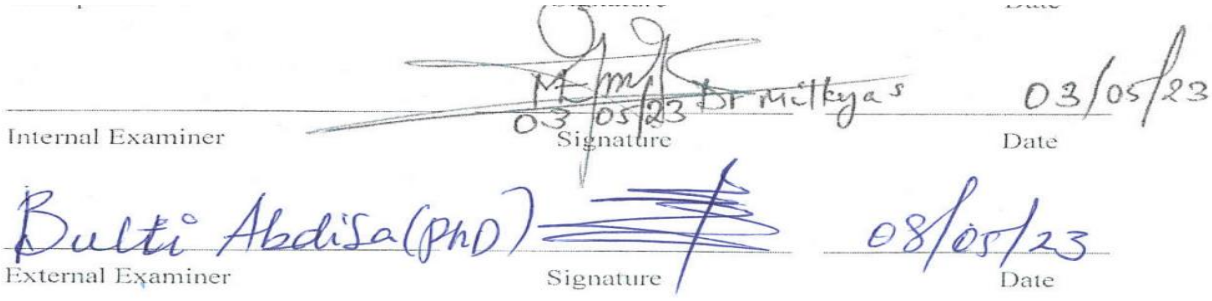

Final approval and acceptance of the thesis are contingent upon the submission of its final copy to the Office of Postgraduate Studies (OPGS) through the Department Graduate Council (DGC) and School Graduate Committee (SGC).

Department Head	Signature	Date
School Dean	Signature	Date
Office of Postgraduate Studies, Dean	Signature	Date

ACKNOWLEDGMENT

First and foremost, I would like to thank the Almighty and merciful God for giving me health, patience, and strength to accomplish this work. I would like to express my deepest gratitude to my advisor Dr. Yadessa Melaku for his kindness, contribution, guidance, advice, and support throughout the research and write-up of the thesis. I would also like to express my gratitude to my co-advisor Dr. Endale Mulugeta for his kindness, unreserved help, and guidance.

I would like to acknowledge the Department of Applied Chemistry for giving me laboratory access and material support. Adama Science and Technology University is duly acknowledged for offering an MSc scholarship opportunity and financial support during my MSc study.

Last but not least, I want to express my gratitude to my family for their continuous support, which enabled me to give all of my academic endeavors my best effort. They have always been the inspiration behind every accomplishment I have made thus far. Without their support, tolerance, and unwavering faith in me, I would not be where I am now.

TABLE OF CONTENTS

CONTENTS PAGES

LIST OF TABLES

LIST OF FIGURES

LIST OF ABBREVIATIONS

ADMET	Absorption, Distribution, Metabolism, Extraction, and Toxicity
ATCC	American-type culture collection
DMSO	Dimethylsulphoxide
DNA	Deoxyribonucleic acid
DEPT	Distortion less Enhancement by Polarization Transfer
DPPH	1,1-diphenyl-2-picryl-hydrazyl
EC_{50}	Half-maximal effective concentration
FDA	Food and Drug Administration
GC-MS	Gas Chromatography-Mass Spectrometry
IC_{50}	Half-maximal inhibitory concentration
MHA	Muller Hinton Agar
MIC	Minimum Inhibition Concentration
NMR	Nuclear Magnetic Resonance
TLC	Thin Layer Chromatography
UV-Vis	Ultraviolet Visible
WHO	World Health Organization

ABSTRACT

*Natural products generated from medicinal plants are among the most recent approaches in the production of herbal product-based drugs owing to high efficacies and fewer adverse effects. Scadoxus multiflorus (Amaryllidaceae) is a widespread ornamental plant of tropical east and South Africa. It is traditionally used for the treatment of many respiratory problems (bronchitis, asthma, pneumonia, sinusitis, etc., and even tuberculosis), scabies, dropsy, and wound healing. The root of the Scadoxus multiflorus (400 g) was successively extracted with n-hexane, chloroform, and methanol to afford 1.00, 1.13, and 12.25% yields respectively. Silica gel column chromatographic separation of the n-hexane and chloroform extract afford five compounds identified as β-sitosterol (**29**), 11-hentriacontene (**30**), 5, 12-henicosadiene (**31**), lindcarpine derivatives (**32**), and linolieamide (**33**). The structures of the isolated compounds were characterized using UV-Vis and NMR spectroscopic techniques (^{1}H NMR, ^{13}C NMR, and DEPT-135). The crude extract and isolated compounds were evaluated in vitro for their antibacterial activities using the disc diffusion method against six bacterial strains. Promising inhibition zone values were observed by β-sitosterol **(29)** (15±0.00mm) and 5, 12-henicosadiene (**31**) (15±0.00mm) against S. typhimurium compared to ciprofloxacin (31.3±1.97). Linoliamide (**33**) and β-sitosterol (**29**) had slightly highest scavenging of DPPH free radicals than other isolated compounds but lower scavenging when compared to ascorbic acid. In silico molecular docking analysis revealed that β-sitosterol (**29**) exhibited better docking efficiency (E.coli) enzyme DNA gyrase (-9.1 kcal/mol) and human topoisomerase II β (-9.6 kcal/mol) when compared to Amoxicillin (− 7.6 kcal/mol) and Abiraterone (-11.8 kcal/mol) respectively. This suggests that compounds **29** may be used as potential drug lead candidates.*

***Keywords*:** *S. multiflorus*, phytochemical screening, biological activity

1. INTRODUCTION

1.1 Background of the Study

Plants have been an important source of medicine for thousands of years. Even nowadays it is thought that plants are the iron hand of medicine since they are still taken by a huge portion of the world's population, particularly in developing countries (Akhlas *et al*., 2021). According to the World Health Organization (WHO) traditional medicine strategy 2002–2005, up to 80% of the African population use traditional remedies such as herbs as their primary source of medicine (WHO, 2002). The medicinal value of these plants is due to the presence of a variety of secondary metabolites such as alkaloids, flavonoids, terpenoids, etc. which are produced by the plant to protect itself from abiotic (drought, radiation, salinity, etc.), biotic stresses (such as bacterial, viral, fungal infections, and attacks by nematodes, mammals, and other animals) and also regulate the mechanisms of flowering, oil production, pollination, and pigment production (Ateş & Yalçin, 2022). These active components are synthesized naturally in all parts of the plant body tissue including bark, root, leaves, stem, flower, fruits, and seeds and they are capable of exhibiting a variety of biological activities including antiviral, antibacterial, anticancer, antioxidants, etc (Ugochukwu, 2013).

These organic compounds from natural sources provide an important foundation as potential lead compounds for the development of new and more effective drugs through structural modification with improved drug ability. They are seemed to exhibit greater biological friendliness and drug-likeness than those derived from purely synthetic sources (Najmi *et al*., 2022). Despite the current preoccupation with synthetic chemistry as a vehicle to discover and manufacture drugs, the contribution of plants to disease treatment and prevention is still enormous (Veeresham, 2012). Until now about one-third of the best-selling drugs in the world are natural products or their derivatives. According to Newman and Cragg 2016, among 1,562 drugs approved by FDA, 64 (4%) were unaltered natural products, 141 (9.1%) were botanical drugs (mixture), 320 (21%) were natural product derivatives and 61 (4%) were synthetic drugs but with natural products pharmacophore (Calixto, 2019).

Ethiopia is one of the six plant biodiversity-rich countries in Africa (Abate *et al*., 2022). The country has a vast diversity of plant species due to the presence of varied topographical settings ranging from the highest peak to a deep valley. There are many plant species in the country, with 12% of them being endemic and over 800 species claiming to treat over 300

diseases (Tadesse *et al*., 2018). The Amaryllidaceae family is one of them. This family is known as one of the top 20 alkaloid-producing plant families. Up to now, more than 600 structurally different alkaloids have been identified from plants in this family, with a variety of pharmacological effects including anticancer, antifungal, antibacterial, antiviral, antimalarial, analgesic, and anti-neurodegenerative capabilities (Koutova *et al*., 2020).

Scadoxus is one of the genera found in the family Amaryllidaceae, comprising about 12 species in the world. Among those species, *S. multiflorus* is one of them. It is an ornamental plant with brilliantly colored flowers that can naturally be found in Southern and tropical Africa (Monkheang *et al*., 2016). Traditionally this plant is used for the treatment of sinusitis, bronchitis, asthma, pneumonia, scabies, dropsy, and wound healing. A preliminary phytochemical analysis of its bulb and leaf extract showed the presence of various secondary metabolites such as flavonoids, alkaloids, cardiac glycosides, tannins, and saponins (Das *et al*., 2021). Thus this study was to investigate the phytochemical, biological, and *in silico* molecular docking study of root extracts and isolated compounds of *S. multiflorus*.

1.2 Statement of the Problem

Most bacterial infections have proven the ability to evolve resistance to antimicrobial drugs that are commercially accessible and every year, antimicrobial resistance kills 700,000 people, with the number expected to rise to 10 million by 2050. As a result, researchers are prompted to look for new, inexpensive, and effective antimicrobial medicines with lesser side effects (Tagliabue & Rappuoli, 2018). Plant-derived phytochemicals found in medicinal plants are effective against a variety of ailments and can be used in environmentally friendly ways. *S. multiflorus* is a good source of phytochemical moieties such as alkaloids, tannins, saponins, steroids, glycosides, flavonoids, and reducing sugar. It has anti-mycobacterial, anti-bacterial, and cytotoxic effects, however, Scientific reports on this medicinal herb are very few therefore, searching for its possible other biological properties is needed (Akhlas *et al*., 2021). To the best of our knowledge, there has never been a systematic biological examination, chemical isolation, or docking study of the constituents of *S. multiflorus* root extracts in Ethiopia. Thus, this study aims to identify the chemical constituents of the roots of *S. multiflorus*, assess the biological activities of extracts as well as isolated compounds, and study *in silico* molecular docking.

1.3 Objectives of the Study

1.3.1 General objective

The overall objective of this study is to isolate and study the biological activities of the root extract of *S. multiflorus.*

1.3.2 Specific objectives

The specific objectives of the study are as follows:

- To extract the root of *S. multiflorus* using n-hexane, chloroform and methanol solvents;
- To isolate chemical constituents from the crude extracts using the silica gel column chromatography technique;
- To elucidate the structure of isolated compounds using the spectroscopic method UV-Vis and (^{1}H NMR, ^{13}C NMR, and DEPT-135) and compare it with literature data;
- To test the antibacterial activities of the extracts and isolated compounds using the disk diffusion method against selected bacterial strains *Escherichia coli, Staphylococcus aureus, Enterococcus faecalis, Pseudomonas aeruginosa, Klebsiella pneumonia, and Salmonella typhimurium;*
- To evaluate the radical scavenging activities of extract and isolated compound using DPPH assay;
- To conduct *in silico* molecular docking study of isolated compounds using AutoDock vina 4.2 against *E. coli* DNA gyrase *S. aureus* pyruvate kinase and human topoisomerase IIβ protein targets;
- To evaluate ADMET prediction by SwissADME, PreADMET, and OSIRIS property predictions.

1.4 Significance of the Study

This study is expected to provide:

- Detailed information about chemical constituents and biological activity of *S. multiflorus*;
- Information about the antibacterial activities of extracts and isolated compounds;
- The result of this study may be valuable in the search for a medication to treat a variety of infections, as well as in drug design and development as a lead compound;
- Information on molecular docking analysis to have a better understanding of the molecular mechanisms of interaction between the compounds with promising activity on target protein of selected organism;
- Documentary information may be referred to by other researchers interested to study on the plant.

2. LITERATURE REVIEW

2.1 Family Amaryllidaceae

Amaryllidaceae also known as Amaryllis (Latin name for a country girl) is a family of monocotyledonous plants that have underground or aerial bulbs (rarely rhizomatous) with large showy and attractive flowers. It was founded in 1805 and now has approximately 1,600 species, 75 genera, 17 tribes, and three subfamilies: Agapanthoideae, Allioideae, and Amaryllidoideae (Fishchuk & Odintsova, 2021). Among them, four genera are indigenous in Ethiopia and Eritrea: *Scadoxus*, *Crinum*, *Ammocharis*, and *Pancratium* (Demissew & Nordal, 2010). Amaryllidaceae are widely distributed across tropical and subtropical zones, with a smaller distribution in temperate areas. The majority of genera can be found in Central and South America, as well as Southern Africa and the Mediterranean (Koutova *et al*., 2020).

The Amaryllidaceae are terrestrial, rarely aquatic or epiphytic, and perennial herbaceous plants that can grow up to 2 m in height (Fishchuk & Odintsova, 2021). The stems are bulbs, covered by membranous leaf bases, the "tunica." The leaves are simple, undivided, spiral or distichous, sheathing or not, sessile or petiolate, and parallel-veined. The inflorescence is a terminal, scapose umbel (derived from condensed, monochasial cymes, sometimes termed a "pseudo-umbel"), rarely of solitary flowers, with bracts present, enclosing the flower buds. The flowers are bisexual, actinomorphic or zygomorphic, pedicellate or sessile, bracteate, epigynous to epiperigynous. Anther**s** are usually dorsifixed, longitudinal (rarely poricidal), and introrse in dehiscence. The gynoecium is syncarpous, with an inferior ovary, carpels, and locules. Placentation is axile or basal; ovules are anatropous, bitegmic, unitegmic, or ategmic. The fruit is a loculicidal capsule or rarely a berry. The seed**s** are phytomelaniferous (Meerow & Snijman, 1998; Simpson, 2010).

2.2 Genus *Scadoxus*

The genus *Scadoxus* belongs to the Haemantheae tribe of the Amaryllidoideae subfamily, which comprises six genera (*Scadoxus, Cyrtanthus, Haemanthus, Clivia, Gethyllis, and Apodolirion*) (Fishchuk & Odintsova, 2021; Francesc *et al.*, 1997). *Scadoxus* was previously classified as part of the genus *Haemanthus*, however, due to differences based on the stems of the species, it was split into two genera. *Scadoxus* currently includes species with elongated stems, whereas *Haemanthus* species have broad stemless leaves (Naidoo, 2016).

According to the World Checklist of Selected Plant Families, there are currently nine accepted species of *Scadoxus*, excluding hybrids and variations (Bødker, 2020). Among these, three species occur in Ethiopia (*S. multiflorus, S. puniceus,* and *S. nutans*) (Demissew & Nordal, 2010). All species names, distribution, and habitat are summarized in **Table 1**.

Table 1: Different species of the genus *Scadoxus* and their distribution and habitat (Bødker, 2020)

Species name	Distribution and habitat
Scadoxus cinnabarinus (Decne.) Friis & Nordal	Sierra Leone to Uganda and part of Central Africa. Lowland forest, riverine forest, or mixed deciduous, high evergreen forest, from near sea level up to 1400 m
Scadoxus cyrtanthiflorus (C.H.Wright) Friis & Nordal	East and Central Africa In dense upland rainforest, ground or epiphytic; 1600-3200 m
Scadoxus longifolius (De Wild. & T.Durand) Friis & Nordal	South Africa and Central Africa Rainforest
Scadoxus membranaceus (Baker) Friis & Nordal	South Africa and part of Portugal and Belgium Coastal forest
Scadoxus multiflorus (Martyn) Raf.	Eastern and Southern Africa, the Arabian Peninsula, and part of Southeast Asia Grassland, wooded grassland, woodland, riverine vegetation, coastal rocks, and montane forest.
Scadoxus nutans (Friis & I.Bj¢rnstad) Friis & Nordal	Ethiopia, Central Africa, Namibia, Nigeria

	Evergreen mountain rainforests, between 1000-2500 m.
Scadoxus pole-evansii (Oberm.) Friis & Nordal	Zimbabwe and South Africa Evergreen moist forest; 1800 m.
Scadoxus pseudocaulus (I.Bjȩrnstad & Friis) Friis & Nordal	Central Africa From sea level and up to 1400 m in regions of high rainfall – rainforest
Scadoxus puniceus (L.) Friis & Nordal	South Africa and part of Ethiopia Montane forest, woodland, on-ground or epiphytic; 1000-2700 m.

The genus *Scadoxus* is characterized by actinomorphic flowers, funnel form to salverform, with perigonium segments equal to or longer than the tube. The stamens are free, and the stigma is undivided. There are just a few ovules per locule. The berry is ovoid to globose and red. The seeds are ovoid and ivory-colored (Fishchuk & Odintsova, 2021). The genus has evolved rhizomatous bulbs and, in some cases, just rhizomes depending on the habitat in which it grows, demonstrating the genus's very adaptable nature in nature. As a result, *Scadoxus* species from the rainforest are distinctly rhizomatous, whilst those from Sub-Saharan Africa exhibit rhizomatous bulbs (Kwembeya, 2021).

2.2.1 Ethnobotanical use of genus Scadoxus

S. multiflorus has a reputation for being toxic because it contains toxic alkaloids like lycorine. As a result, animals including goats, sheep, and cows are adversely affected by these plants. The plant's leaves and bulbs are exceedingly toxic, commonly killing domestic and experimental animals. As a result, it is used as an arrow poison and fish-killing poison in tropical Africa (Akhlas *et al*., 2021). However, this herb has been used in South Africa for the treatment of various diseases, including leprosy, ulcers, febrile colds, asthma, coughs, dropsy, scabies, and wounds. In Kenya, used in the treatment of respiratory problems including asthma, bronchitis, tuberculosis, pneumonia, and sinusitis. This can be accomplished by boiling the tuber and then drinking the resulting liquid after it cools (Mwamidi *et al*., 2012). In Eastern Tanzania, a bath with root infusion of this plant is used to treat mental illness

(Chhabra *et al*., 1987). In Ethiopia, the root of this plant is also used to treat internal cancer in combination with other herbs and applied topically (Abate *et al*., 2022; Tuasha *et al.*, 2018).

2.2.2 Chemical constituents of genus *Scadoxus*

In 1987 Ali *et al.*, isolate and characterize three alkaloids lycorine (**1**), galanthamine (**2**), and sanguinine (**3**) for the first time from the bulb of *S. multiflorus* (Ali *et al*., 1987). Abdallah *et al*., (1989) isolated lycorine (**1**), galanthamine (**2**), 2-O-acetylchlidanthine (**4**), haemultine (**5**), and hippadine (**6**) from the bulb of *S. multiflorus* (Abdallah *et al*., 1989).

Pagning *et al*., (2016) isolated six compounds (**7**-**12**): sideroxylin (**7**), 5-hydroxymethyl-2-furancarboxaldehyde (**8**), C-6,O-7-dimethyldenaromadendrin (**9**), 4-(hydroxymethyl)-5 hydroxy-2H-pyran-2-one (**10**), 7-deoxy-transdihydronarciclasine or trans-dihydrolycoricidine (**11**) and farrerol (**12**) from the root of *S. pseudocaulus* (Pagning *et al*., 2016).

Yokosuka *et al*., (2017) isolate ten (**13–22**) phenolic glycosides from the bulbs of *S. multiflorus*. 2,4-Dihydroxy-6-methoxy-3-methylacetophenone 4-O-*α*-Lrhamnopyranosyl-(1→6)-*β*-D-glucopyranoside (**13**), 2,4-Dihydroxy-6-methoxy-3-methylacetophenone 4-O-*β*-Dapiofuranosyl-(1→6)-*β*-D-glucopyranoside (**14**), 2,4-Dihydroxy-6-methoxy-3-methylacetophenone 4-O-*β*-Dglucopyranosyl-(1→6)-*β*-D-glucopyranoside (**15**), 2,4-Dihydroxy-6-methoxyacetophenone 4-O-*β*-D-glucopyranosyl-(1→6)-*β*-D-glucopyranoside (**16**), 2,4-Dihydroxy-6-methoxyacetophenone 4-O-*α*-L-arabinopyranosyl-(1→6)-*β*-D-glucopyranoside (**17**), 3,5-Dimethoxyphenyl 1-O-*α*-L-arabinopyranosyl-(1→6)-*β*-Dglucopyranoside (**18**), 2,4-dihydroxy-6-methoxyacetophenone 4-O-*α*-L-rhamnopyranosyl-(1→6)-*β*-D-glucopyranoside (**19**), 2,4-dihydroxy-6-methoxyacetophenone 4-O-*β*-D-apiofuranosyl-(1→6)-*β*-D-glucopyranoside (**20**), 2,6-dimethoxy acetophenone 4-O-*β*-D-glucopyranoside (**21**), and 4,6- dimethoxy acetophenone 2-O- *β*-D-glucopyranoside (**22**) (Yokosuka *et al*., 2017).

Naidoo *et al*., (2017) isolated two alkaloids haemanthamine (**23**) haemanthidine (**24**), and metolachlor (**25**), the first chlorinated amide in the Amaryllidaceae family from the bulbs of *S. puniceus* (Naidoo *et al*., 2017).

The GC/MS analysis of ethanol crude of the bulb *S. multiflorus* showed the presence of two alkaloids montanine (**26**) 92% and undulatine (**27**) 8%, which showed potent inhibitory

activity better than the standard galanthamine (Cahlíková *et al.*, 2011). In another research article, the isolation of a novel plant protein xylanase, and *α*-amylase inhibitory protein, known as XAIP were reported from the bulb of *S. multiflorus* (Kumar, 2010).

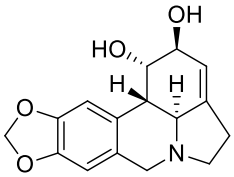

1

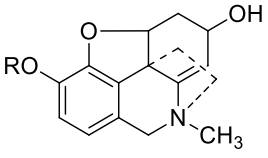

2 = **R = CH$_3$**
3 = R = H

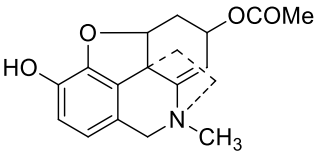

4

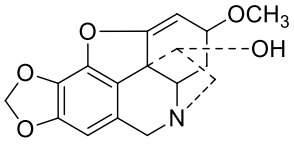

5

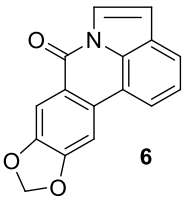

6

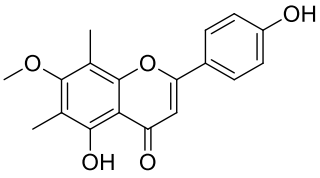

7

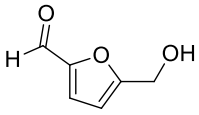

8

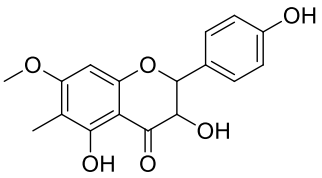

9

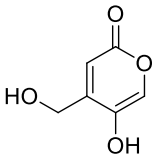

10

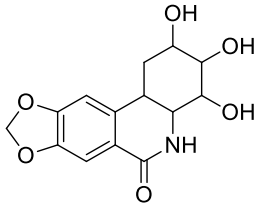

11

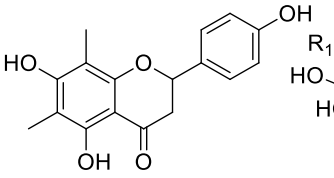

12

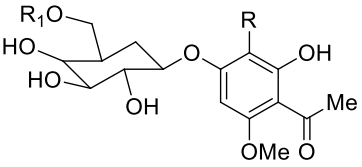

	R	R_1
13	Me	Rha
14	Me	Api
15	Me	Glc
16	H	Glc
17	H	**Ara**

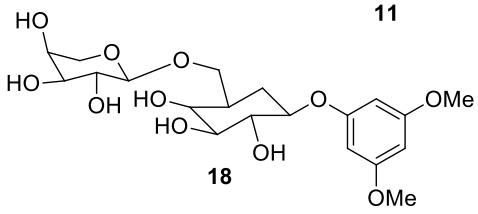

18

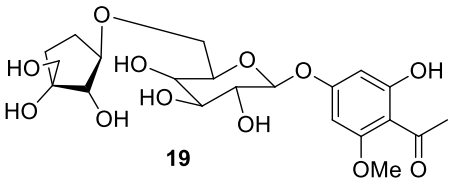

19

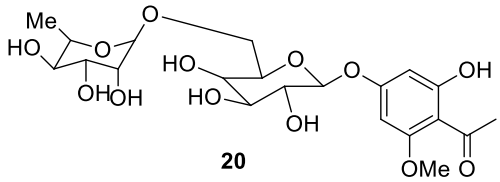

20

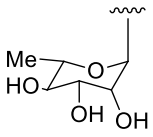

Rha

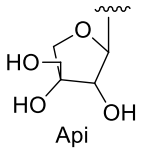

Api

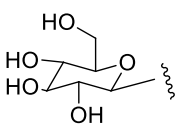

Glu

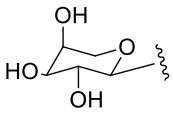

Ara

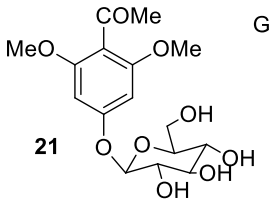

21

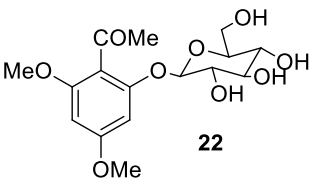

22

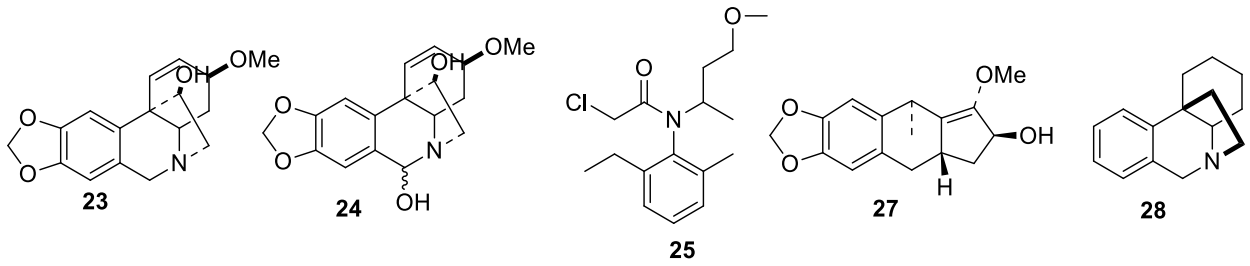

Figure 1: Chemical constituents of genus *Scadoxus*

2.2.3 Pharmacological study of *Scadoxus*

Traditionally *S. multiflorus* is used in the treatment of coughs, wounds, and various gastrointestinal problems. Cahlíková *et al*., (2011) mentioned that the GC/MS analysis of ethanol crude of the bulb of *S. multiflorus* showed the presence of two alkaloids montanine (**27**) 92% and undulatine (**28**) which showed potent activity against butyrylcholinesterase (HuBuChE) inhibition activity better than the standard galanthamine with an IC_{50} value of 54.3 ± 3.1 µg/mL (Cahlíková *et al*., 2011).

Adewusi and Steenkamp (2011**)** reported on the strong acetylcholinesterase (AChE) inhibitory activity with an IC_{50} value of 0.0003 mg/mL from ethyl acetate extract of *S. puniceus* bulb (Adewusi & Steenkamp, 2011).

Seoposengwe *et al*., (2013) determined the cytotoxicity of bulb extracts of *S. puniceus* against inhibiting rotenone-induced caspase-3 with LC_{50} 20.75±1.47 µg/mL. The authors revealed that pre-treating cells with *S. puniceus* extracts reversed the effects of rotenone on intracellular ROS levels and also rotenone exposure decreased intracellular glutathione levels that suggesting the species may possess neuroprotective properties (Seoposengwe *et al*., 2013).

Pagning *et al*., (2016) evaluated the extracts and isolated compounds from *S. pseudocaulus* for antimicrobial, free radical scavenging, and butyrylcholinesterase (BuChE) inhibition activities. The ethyl acetate extraction (MIC = 64 –512 µg/mL) and farrerol (**12**) (MIC = 2 – 16 µg/mL) showed significant antibacterial activity. Methanol extract shows the strongest antioxidant activity with the lowest IC_{50} value of 7.25 µg. 4-(hydroxymethyl)-5 hydroxy-2H-pyran-2-one (**10**) has shown significant butyrylcholinesterase (BuChE) inhibition activities with IC_{50} value of 23.5 µM (Pagning *et al*., 2016).

Naidoo (2016) evaluated the antioxidant activity, antimicrobial activity, and AChE inhibitory of *S. puniceus* extract. Methanol extract of the leaf showed the strongest radical scavenging activity 91.61% with a lower EC_{50} 0.07 value. The pethreloem extract of the bulb showed the strongest MIC value of 0.39 mg/mL against *K. pneumoniae* and *S. aureus* bacterial strains. The leaf, stem, and basal plate extracts revealed excellent activity against *C. albicans* with MIC values of less than 1 mg/mL. The bulb of *S. puniceus* exhibited the strongest AChE inhibitory activity with IC_{50} value of 0.07 mg/mL (96.58%) (Naidoo, 2016).

Islam *et al*. (2021) examined the aqueous crude extract of the aerial parts of *S. multiflorus* for high concentration-induced toxicity and low concentration-mediated protective characteristics. After 24, 48, and 72 hours, the crude extract from *A. cepa* exhibited concentration-dependent toxicity. The authors state that at low concentrations, the crude extract demonstrated anti-inflammatory, membrane-stabilizing, and anithrombolytic properties. (Akhlas *et al*., 2021).

Das *et al*., (2021) reported the antimitotic and cytotoxic properties of leaf aqueous extract of *S. multiflorus* in *allium cepa* root apical meristem cells. The study shows that the leaf extract treatment (0.25–4 mg mL^{-1}) resulted in both time and concentration-dependent root growth retardation effects. The maximum root growth inhibitory effect (96.71±1.2, 96.97±1.2, and 97.09±1.1% respectively at 24, 48, and 72 h) was observed at its highest concentration (4 mg mL^{-1}). The used lowest concentration (0.25 mg mL^{-1}) also showed a significant (p<0.0001) growth retardation in each data set. The calculated IC_{50} values for root growth retardation assay were 0.74, 0.35, and 0.25 mg mL-1 at 24, 48, and 72 h respectively (Das *et al*., 2021).

Emam *et al*., (2022) reported *in vitro* anticancer activity of the 80% ethanolic extract of 23 traditionally used Ethiopian plants against cervical (HeLa) and prostate (PC3) cancer cell lines by MTT colorimetric assay. Among them, *S. multiflorus* exhibited significant anticancer activity with IC_{50} 14.6 and 9.8 against HeLa and PC3 cancer cell lines respectively (Emam *et al*., 2022).

2.3 *Scadoxus multiflorus*

2.3.1 Botanical description of *S. multiflorus*

S. multiflorus (**Figure 2**) (Vernacular name dem-astefi/ yesetan shunkurt in Amharic and abrasha in Afan Oromo) is a summer-growing deciduous plant with rhizomatous bulbs that produces extremely beautiful flower heads and decorative orange to red berries. The specific nickname '*multiflorus*' means many-flowered, and refers to rich-flowered heads. The flower is known as the football lily, African blood lily, powderpuff lily, pincushion flower, and so on. It was first introduced by Thomas Martyn in 1795 as *Haemanthus multiflorus*. In 1838, Constantine Samuel Rafinesque changed the genus of *H. multiflorus* to a new genus *Scadoxus* (Akhlas *et al.*, 2021). This plant widely grows naturally in sub-Saharan Africa, South Africa, Arabian Peninsula, and Southeast Asia. Also, these species are found in savannah woodlands, riverine and montane forests. It seems to prefer some shade and is growing on dark brown to blackish soils, from 1000 to 3000 m (Pagning *et al*., 2016). It is found in almost all floristic regions within Ethiopia and Eritrea, except in the lowlands. The main flowering period in Ethiopia is from January to April (Demissew & Nordal, 2010).

Figure 2: *S. multiflorus* (Martyn) Raf. (a picture taken by Ilili Dine on August 2022 from Adama)

Table 2: A brief description of the species *S. multiflorus* (Afroz, 2018)

Roots	Rhizomatous bulb, long greenish-white with red maroon spots neck, 3.5-3.0 cm wide, and off-white in color
Leaves	Radical, simple, lanceolate, 10–40 cm, parallel-veined, acute, entire, not distichous, herbaceous in texture, evident middle nerves, always glabrous, appear just after the appearance of the false stem or pseudo stem
Petioles	The bases of the leaves and petioles are

	tightly wrapped together to form a pseudo stem or false stem, 5–60 cm long, purple-spotted
Inflorescence	Umbellate cyme with multiple blooms grown at the apex of a leafless scape, full-bloomed flowers make a globules head that lasts only a week.
Flowers	Actinomorphic, a bisexual, with a greenish-red pedicel which is 3.8 cm long, epigynous, flower head produced directly from the bulb, consisting of hundreds of red florets with yellow tripped stamens, the head is 10-25 cm in diameter
Perianth segments	Petaloid, united below into a tube, reddish-pink, glabrous, tube about 1 cm long.
Stamens	6 spreading petal-like segments, epiphyllous, filaments long about 3.1 cm, anthers linear, about 0.4 cm long, dorsifixed, introrse
Carpels	syncarpous, ovary 3-celled, inferior, about 0.3 cm long, green, placentation axile,
Style	4 cm long from the top of the tube
Fruit	oval-shaped berries, globose, 0.5–1 cm in diameter, bright orange to red in color and become red when ripped

3. MATERIALS AND METHODS

3.1 Plant Material Collection and Identification

The plant material was collected from the Western Hararge Zone, Doba district which is located about 378 km to the east of Addis Ababa. The identification of the plant material was done with the help of Botanist Melaku Wendaferash at the Department of Biology, National Herbarium of Ethiopia, Addis Ababa University with a voucher specimen (ID001).

3.2 Materials and Chemicals

Column chromatography was carried out using silica gel (200-400mesh) ASTM. The ultraviolet and visible (UV-Vis) spectrum was taken on Spectroscopic Genesys™ 2PC UV-Vis scanning spectrometer (200-400 nm) in a solvent at room temperature. Thin Layer Chromatography (TLC) was performed using pre-coated aluminum-backed supported silica gel 60 F254 (0.2 mm thickness). ^{1}H and ^{13}C NMR spectra were recorded on a Bruker Avance 400 MHz spectrometer with TMS as the internal standard and $CDCl_3$ and DMSO-d_6 as a solvent. The Melting point was determined by Cambridge microscopy instruments.

Chemicals that were used for extraction, isolation, phytochemical analysis, and other activities are silica gel (Loba Chemie PVT. LTD., 200-400 mesh), ethanol (Favor trading PLC, 99.9%), methanol (Alpha Chemika, 99.8%), chloroform (Blulux, 99.8%), *n*-hexane (Loba Chemie PVT. LTD., 99%), ethyl acetate (Loba Chemie PVT. LTD., 99.5%), ammonium solution (Avi chem, 25%), ferric chloride (Sigma Aldrich, 97%), sulfuric acid (Loba Chemie PVT. LTD., 98%), hydrochloric acid (Loba Chemie PVT. LTD., 35.4%), DPPH (Sigma Aldrich, 97%), DMSO (Srlchem, 99.5%), Potassium Iodide (Samir Tech-Chem PVT. LTD., 99.8%), Iodine (Alpha Chemika, 98.5%), and distilled water.

3.3 Extraction and Preparation of Plant Material

3.3.1 Preparation of plant material

The collected roots of *S. multiflorus* were cut into smaller pieces and dried under shade. Then it was grounded into a fine powder using a mechanical grinder. The powder was stored in airtight containers at room temperature till further experimentation.

3.3.2 Extraction

Root powder of *S. multiflorus* (400 g) was soaked in *n*-hexane (2 L) for 72 hrs at room temperature and shacked using mechanical shaking. The solution was filtrated and concentrated using a rotary evaporator at a temperature of about 40°C to give *n*-hexane extract. The marc was further extracted in chloroform (2 L) for 72 hrs, filtered, and concentrated to afford chloroform extract. The marc left was soaked in methanol (2L) for 72 hrs, filtered, and concentrated to afford methanol extract. The extracts were analyzed for their TLC profile to select the best solvent for silica gel column chromatography. The extracts were placed in a deep freezer until needed for further experiment.

3.4 Phytochemical Screening Tests

Phytochemical examinations were carried out for methanol extracts as per the standard methods.

Test for Alkaloids (Wagner's test): The methanol extract (30 mg) was separately stirred with 1% HCl (0.5 mL) in a water bath for 5 min and filtered into a test tube. 1 mL of Wagner's reagent (Iodine in Potassium Iodide) was added; the formation of a brown/reddish precipitate indicates the presence of alkaloids (Praiwala *et al*., 2019).

Test for flavonoids: The methanol extract (30 mg) was dissolved in 10 mL of ethyl acetate and heated for 3 min using a steam bath. The mixture was filtered, and to the filtrate 1mL of dilute ammonia solution was added. The formation of intense yellow color ratifies the presence of flavonoids (Mir *et al.*, 2016a).

Test for Phenols: The methanol extract (30 mg) was dissolved in 5mL of distilled water. To this, a few drops of neutral 5% ferric chloride solution was added. A dark green color indicated the presence of phenolic compounds (Bargah & Rohit, 2015).

Test for Tannins: The methanol extract (30 mg) was dissolved in 5mL of distilled water, filtered and ferric chloride reagent was added to the filtrate. A blue-black, green, or blue-green precipitate was taken as evidence of the presence of tannins (Mir *et al*., 2016b).

Test for Terpenoids (Salkowski's Test): The methanol extract (30 mg) was dissolved in 2 mL of chloroform and concentrated H_2SO_4 (3 mL) was carefully added to form a layer. An appearance of reddish brown color on the inner face indicated the presence of terpenoids (Santhi & Sengottuvel, 2016).

Test for saponins: The methanol extract (30 mg) was dissolved in 5 mL of distilled water and shaken while heating to boil. Frothing showed the presence of saponins (Kamal *et al*., 2012).

Test for Steroids: The methanol extract (30 mg) was dissolved in 10 mL of chloroform and an equal volume of concentrated H_2SO_4 was added by the sides of the test tube. A reddish-brown color at the interphase indicates the presence of a steroidal ring (Nwodo & Nkwocha, 2015).

3.5 Isolation of Compounds

The crude extracts of *n*-hexane and chloroform showed a comparable TLC profile. The chloroform crude extract (4 g) was adsorbed on 6 g of silica gel (mesh size 200-400), and subjected to silica gel chromatography (170 g of silica gel using *n*-hexane for packing). To this *n*-hexane crude (4 g) which was dissolved in *n*-hexane was added to the top. The increasing gradient of ethyl acetate in *n*-hexane was used as eluent. A total of 270 fractions were collected (**Table 3**). Fractions that showed similar Rf values were combined.

Table 3: Summary of fractionation of *n*-hexane and chloroform extract

Solvent system	Ratio	Fractions	Volume of fraction (mL)
n-hexane	100	F_1-F_8	100
n-hexane/ ethyl acetate	99:1	F_9-F_{10}	20
	98:2	F_{11}-F_{13}	20
	97:3	F_{14}-F_{24}	20
	96:4	F_{25}-F_{34}	20

	95:5	F_{35}-F_{46}	20
	94:6	F_{47}-F_{52}	20
	93:7	F_{53}-F_{58}	20
	92:8	F_{59}-F_{74}	20
	91:9	F_{75}- F_{79}	20
	90:10	F_{80}-F_{91}	20
	88:12	F_{92}-F_{119}	50
	85:15	F_{120}-F_{134}	50
	80:20	F_{135}-F_{140}	30
	75:25	F_{141}-F_{154}	30
	70:30	F_{155}-F_{160}	30
	65:35	F_{161}-F_{180}	20
	60:40	F_{181}-F_{187}	20
	50:50	F_{188}-F_{195}	20
	40:60	F_{196}-F_{209}	30
	30:70	F_{210}-F_{219}	30
	20:80	F_{220}-F_{224}	50
	90:10	F_{225}-F_{252}	50
Ethyl acetate (EtOAc)	100	F_{253}-F_{270}	100

Fraction 109-119 obtained (eluted with 88 % EtOAc in *n*-hexane) having a similar spot on TLC with two compounds, repacked for re-purification with a small silica gel column (50 g of silica gel) and eluted by isocratic systems using 95% of ethyl acetate in *n*-hexane. A total of 42 fractions were collocated, each 20 mL. From these fractions, 7-11 afforded *β*-sitosterol (**29)** (17 mg) as a white solid, and fractions 35-37 afforded 5, 12-henicosadiene (**31**) (30 mg) as a yellow solid. From fractions 34-37 obtained from fractionation of chloroform and *n*-hexane extract (eluted with 95% EtOAc in *n*-hexane) having a similar spot on TLC with two compounds, repacked for further purification with a small silica gel column (50 g of silica gel) and eluted by isocratic systems using 95% of ethyl acetate in *n*-hexane. A total of 36 fractions were collocated, each 20 mL. Fraction 31 afforded 11-hentriacontene (**30**) (32 mg) as a pale yellow muddy solid. A fraction from 190-197 obtained from fractionation of chloroform and *n*-hexane extract (eluted with 50% EtOAc in *n*-hexane) afforded lindcarpine derivatives (**32**) (36 mg) as a reddish brown solid. A fraction from 170-177 obtained from

fractionation of chloroform and *n*-hexane extract (eluted with 65% EtOAc in *n*-hexane) afforded linolieamide (**33**) (30 mg) as a yellow solid.

3.6 Structural Elucidation

The UV-Vis and NMR spectroscopic techniques were employed to elucidate the structure of isolated compounds. The ^{1}H NMR, ^{13}C NMR, and DEPT were obtained using Bruker Avance 400 MHz spectrometer.

3.7 Biological Activity

3.7.1 Antibacterial Activity

In vitro antibacterial activity of extracts and isolated compounds of S. *multiflorus* was studied against six pathogenic bacterial strains *Escherichia coli* (ATCC 25922), *Staphylococcus aureus* (ATCC 25923), *Enterococcus faecalis* (ATCC 29212), *Pseudomonas aeruginosa* (ATCC 27853), *Klebsiella pneumonia* (ATCC 700603), and *Salmonella typhimurium* (ATCC 13311) using the disc diffusion method. The standard drug (ciprofloxacin) as a positive control and dimethyl sulfoxide (DMSO) as negative control were used. Then the sets of four dilutions (100, 50, 25, and 12.5 mg/mL) for crude extract and (10, 5, 2.5, 1.25 mg/mL) for isolated compounds were prepared. The strains of bacteria were adjusted at 1.5×10^{8} colony forming units (CFU/mL). Muller Hinton Agar plates were inoculated by streaking swabs over the entire sterile agar surface and the procedure was repeated 2 more times rotating the plates at 60˚ each time to ensure even distribution and the rim of the plates was swabbed. After allowing the inoculum to dry for 10 mins at room temperature (rt), sterile filter paper disks (Whatman No. 1, diameter = 6 mm) were placed on the inoculated plates. From each dilution, 20µL were taken and dispensed on the filter papers and allowed to stand at rt for 30 mins, then incubated at 37˚C for 24hrs. Afterward, the zone of growth inhibition (including the diameter of the disk) of the extracts and isolated compounds were measured in mm and compared with the standard drugs. A zone of inhibition ≥9–15 mm is an indication of strong antimicrobial activity (Rani & Khullar, 2004).

3.7.2 Antioxidant Activity

The free radical scavenging activity of the extracts and isolated compounds was measured through the 1,1-diphenyl-2-picryl-hydrazyl (DPPH) method by measuring the absorbance of

DPPH at 517 nm. The crude extracts and isolated compounds were diluted in four vials as 1000, 500, 250, and 125 µg/mL (crude extracts) and 100, 50, 25, and 12.5 µg/mL (isolated compounds). To each 1 mL of the above solutions, 4 mL of 0.04% DPPH (prepared in methanol by dissolving 4 mg DPPH in 100 mL methanol) were added to give 200, 100, 50, 25 µg/mL (crude extract) and 20, 10, 5, 2.5 µg/mL (isolated compounds). The resulting solution was placed for 30 minutes in the dark and then subjected to a UV-Vis spectrophotometer to record absorbance at 517 nm. The capability to scavenge the DPPH radical was calculated using the following equation (Brand-Williams *et al*., 1995):

$$\% \text{ of radical scavenging activity} = \frac{Ab_{standard} - Ab_{analyte}}{Ab_{standard}} \times 100$$

3.8 *In Silico* Molecular Docking Studies of Isolated Compounds

3.8.1 Preparation of ligands

The 2D structures (.mol) of all isolated compounds were drawn and each individual structure was analyzed by using ChemDraw 16.0. Energy of each molecule was minimized using ChemBio3D. The 3D coordinates (.PDB) of each molecule was obtained through optimized structure.

3.8.2 Preparation of macromolecules

The crystal structure of receptor molecules *S. aureus* Pyruvate Kinase (PDB ID 3T05), human topoisomerase IIβ with DNA (PDB ID 3QX3), and *E. coli* Gyrase B (PDB ID 7P2W) were downloaded from protein data bank. The protein preparation was done using the reported standard protocol by removing the co-crystallized ligand, selected water molecules and cofactors, the target protein file was prepared by leaving the associated residue with protein by using Auto Preparation of target protein file Auto Dock 4.2.6 (MGL tools 1.5.6).

3.8.3 Autodock Vina analysis

The graphical user interface program Auto Dock 4.2.6 was used to set the grid box for docking simulations. The grid was set so that it surrounds the region of interest in the macromolecule. The docking algorithm provided with Auto Dock Vina was used to search

for the best-docked conformation between ligand and protein. During the docking process, a maximum of nine conformers were considered for each ligand. The conformations with the most favorable (least) free binding energy were selected for analyzing the interactions between the target receptor and ligands by Discovery studio visualizer and PyMOL.

AutoDock Vina with standard protocol was used to dock the protein *S. aureus* Pyruvate Kinase (PDB ID 3T05), human topoisomerase IIβ with DNA (PDB ID 3QX3), and *E. coli* Gyrase B (PDB ID 7P2W) and isolated ligands into the active site of proteins. The molecular docking studies were carried out using AutoDockTools (ADT), which is a free graphic user interface (GUI) for the AutoDock Vina program. The grid box was constructed using 30x30x30, pointing in x, y, and z directions, respectively, with a grid point spacing of 0.375 Å. The center grid box is 17x29x21 Å for 3T05, 27x103x36 Å for 3QX3, and -28x7x0.816 for 7P2W. Nine different conformations were generated for each ligand scored using AutoDock Vina functions and were ranked according to their binding energies. The ligands are represented in different color, H-bonds and the interacting residues are represented in stick model representation.

3.9 *In silico* Drug-Likeness and Toxicity Predictions

The isolated compounds were evaluated for their pharmacokinetic profiles by *in*-silico methods for predicting their molecular properties using Lipinski's Rule of Five. The structures of isolated compounds were drawn using ChemDraw software and converted to their canonical simplified molecular-input line-entry system (SMILE). They were uploaded to the PASS prediction website where the predicted activities and their corresponding Pa values were obtained. In silico pharmacokinetics, ADME (Absorption, Distribution, Metabolism, Excretion), and properties of the compounds were estimated using SwissADME and PreADMET tools. This ADME properties prediction provides valuable data to select better preclinical candidates. Also, the organ toxicities and toxicological endpoints of the isolated compounds were predicted using PreADMET and OSIRIS properties (Anza *et al*., 2021).

4. RESULTS AND DISCUSSION

4.1 Extraction Yield

S. multiflorus root were extracted using *n*-hexane, chloroform and methanol to afford 4 g (1%), 4.5 g (1.125%), and 49 g (12.25%) crude extracts, respectively. According to Truong *et al*., (2019) methanol is the most effective solvent for extraction, resulting in the highest extraction yield (Truong *et al*., 2019), and *n*-hexane is used for the extraction of non-polar compounds. Thus these results show that a better extractive yield was obtained from the methanol extract and also reveal that the secondary metabolites present in the root of *S. multiflorus* are mainly polar.

4.2 Phytochemical Screening

Phytochemical screening tests were performed to determine the class of chemicals present in the crude extracts. The result shows the presence of alkaloids, flavonoids, tannins, steroids, saponins, and terpenoids except phenol (**Table 3**) in agreement with Mariita *et al* (2011) who reported the presence of alkaloids, flavonoids, tannins, terpenoids saponins, glycoside, and reducing sugar from methanol extract of the root of *S. multiflorus* (Mariita *et al*., 2011). The results obtained suggest that detected phytochemicals may be the bioactive constituents of this plant suggesting the plant is a valuable reservoir of bioactive compounds with significant medical value.

Table 3: Phytochemical screening tests on the root extract of *S. multiflorus*

Sample	**Secondary metabolites**	**Test**	**Observation**
Methanol	Alkaloid	Wagner's test	+
	Flavonoids	Alkaline test	+
	Phenol	Ferric chloride test	-

extract	Tannins	Ferric chloride test	+
	Terpenoids	Salkowski's Test	+
	Saponins	Froth Test	+
	Steroid	Salkowski's Test	+

+ shows presence, -shows absence

4.3 Characterization of Compounds

β-sitosterol (**29**) (19 mg) was isolated as a white solid with R_f value of 0.63 (80% EtOAc in *n*-hexane as eluent). The ^{1}H NMR spectrum (Appendix 1) showed the presence of six methyl signals that appeared as two methyl singlets at *δ* 0.70 (s, 3H, H-18), and 1.03 (s, 3H, H-19) which corresponds to the angular methyl singlets. Three methyl doublets appeared at *δ* 0.95 (d, 3H, H-21), 0.88 (d, 3H, H-26), and 0.86 (d, 3H, H-27), and a methyl triplet at *δ* 0.80 (t, 3H, H-29). The signal at *δ* 2.37 (d, 2H, H-4) and 2.30 (t, 2H, H-7) revealed that the two methylene adjacent to carbon attached to a hydroxyl group. The signal at *δ* 3.55 (m, 1H, H-3) is due to Sp^3 oxygenated methane bearing to the hydroxyl group. Also, one olefinic proton was shown at *δ* 5.37 (dd, 1H, H-6) as a doublet of doublet.

The ^{13}C NMR spectrum with the aid of DEPT-135 (Appendix 2 and 3) showed twenty-nine carbon signals made up of six methyls, eleven methylenes, nine methine, and three quaternary carbon signals. The signals at *δ* 140.7 (C-5) and 121.7 (C-6) correspond to olefinic double bonds of which the former one is Sp^2 quaternary carbon. The signal at *δ* 71.8 (C-3) is assignable to methine carbon bearing. The signals at *δ* 11.8 (C-19) and 19.4 (C-18) correspond to angular methyl carbon atoms C_{19} and C_{18} respectively. The chemical shift value for C_{18} is lower due to *γ*-gauche interaction that increases the screening of the C_{18}. From the above spectral data and comparison with the literature, the structure of the compound was identified as *β*–sitosterol (**29**). It is widely distributed in plants and is the commonest sterol of higher plants. Previously isolation of *β*–sitosterol (**29**) from the methanol extract of *Lycoris radiata* (Amaryllidaceae) was reported but, this is the first time it isolated from the genus *Scadoxus*. *β*–sitosterol (**29**) is known to possess various biological activities such as antinociceptive, immunomodulatory activity, antimicrobial, anticancer, anti-diabetic activity, and antioxidant (Babu & Jayaraman, 2020).

Table 4: ^{1}H and ^{13}C NMR spectral data of *β*-sitosterol (**29**)

	β-sitosterol (**29**)		(Aliba *et al*., 2018)	
Position	δ_H in ppm	δ_C in ppm	δ_H in ppm	δ_C in ppm
1	1.35 (t, 2H)	37.2		37.3
2	1.55 (m, 2H)	31.9		31.7
3	3.55 (m, 1H)	71.8	3.55 (m, 1H)	71.9
4	2.37 (d, 2H)	42.3		42.3
5	-	140.7		140.8
6	5.37 (dd, 1H)	121.7	5.37 (dd, 1H)	121.8
7	2.30 (t, 2H)	31.9		32.0
8	1.97 (m, 1H)	29.1		29.3
9	1.85 (d, 1H)	50.1		50.2
10	-	36.5		36.6
11	2.05 (m, 2H)	21.0		21.2
12	1.51 (t, 2H)	39.7		39.9
13	-	42.3		42.3
14	1.88 (m, 1H)	56.7		56.9
15	1.33 (m, 2H)	23.0		23.2
16	1.30 (m, 2H)	28.2		28.3
17	2.01 (m, 1H)	56.0		56.2
18	0.70 (s. 3H)	11.9	0.70 (s, 3H)	12.1
19	1.03 (s, 3H)	19.4	1.03 (s, 3H)	19.1
20	1.55 (m, 1H)	36.1		36.2
21	0.95 (d, 3H)	18.7	0.95 (d, 3H)	18.9
22	1.27 (m, 2H)	33.9		34.0
23	1.18 (m, 2H)	24.3		24.4
24	1.33 (m, 1H)	45.8		45.9
25	1.51 (m, 1H)	28.2		26.2
26	0.88 (d, 3H)	19.4	0.87 (d, 3H)	19.9
27	0.86 (d, 3H)	19.0	0.85 (d, 3H)	19.1
28	1.05 (d, 2H)	23.0		22.8
29	0.80 (t, 3H)	11.8	0.84 (t, 3H)	9.6

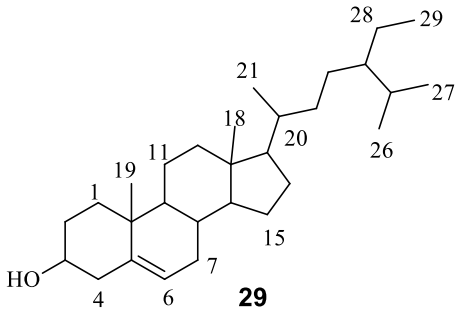

Figure 3: Structure of β –sitosterol

11-hentriacontene (**30**) (32 mg) was isolated as a pale yellow muddy solid with R_f value of 0.54 (90%EtOAc in *n*-hexane as eluent). The ^{1}H NMR (Appendix 4) spectral data showed the corresponding signals of the olefinic protons with chemical shifts δ 5.4 (m, 2H, H-11 & H-12) as a multiplet. The multiplet signal at δ 2.38 (m, 4H, H-10 & H-13) are integrated due to the methylene protons allylic to double bonds. An up-field proton triplet signal at δ 0.90 (t, 6H, H-1 & H-31) is evident for the presence of terminal methyl proton in the compound.

The ^{13}C-NMR spectrum with the aid of DEPT-135 (Appendix 5 and 6) displayed two sp^2 methines at δ 130.0 (C-11) and 129.7 (C-12). In addition, peaks at δ 22-34.1 correspond to the methylene groups of which the deshilded appeared at δ 34.1 (C-10 & C-13) suggesting methylene next to sp^2 methines. Whereas the methylene that appeared at δ 31.0 is attributed to methylene at C_3 and C_{29}. The more intense signal at δ 29.6 represented the existence of many overlapped methylene carbons. The most up-field carbon signal at δ 14.1 (C-1 & C-31) accounts for the presence of terminal methyl protons. The above spectral data suggest that the compound is 11-hentriacontene (**30**), which was previously isolated from GC-MS analysis of hexane extract of *Cleisostoma scolopendrifolium* flower (Son *et al*., 2020) and also isolated from flowers of *Inula grantioides* (Burdi *et al*., 1991; Gashu, 2018). It is used in mating stimulant pheromone of *Fannia femoralis* and plays a key role in the pollination mechanism between *Cleisostoma orchids* and *Megachile bees* (Son *et al*., 2020). This is the first time 11-hentriacontene (**30**) isolated from *S. multiflorus* and reported herein for the first time from genus.

Table 5: ^{1}H and ^{13}C NMR spectral data of 11-hentriacontene (**30**)

Position	δ_H(δ in ppm)	^{13}C NMR (δ_C in ppm)	DEPT-135 (δ_C in ppm)

C_1 & C_{31}	0.9 (t, 6H)	14.1	14.1
C_2 & C_{30}	1.2 (m, 4H)	22.7	22.7
C_3 & C_{29}	1.6 (m, 4H)	31.9	31.9
C_4 & C_{28}	1.2 (m, 4H)	29.3	29.4
C_5-C_8, C_{15}-C_{27}	1.3 (m, 34H)	29.6	29.6
C_9 & C_{14}	2.0 (m, 4H)	29.7	29.7
C_{10} & C_{13}	2.3 (m, 4H)	34.1	34.1
C_{11}	5.4 (m, 1H)	130.0	130.0
C_{12}	5.4 (m, 1H)	129.7	129.7

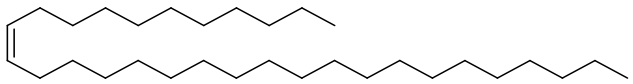

30

Figure 4: Structure of 11-hentriacontene

5, 12-henicosadiene (**31**) (30 mg) was isolated as a yellow solid with R_f value of 0.44 (90%EtOAc in *n*-hexane as eluent). The ^{1}H NMR (Appendix 7) spectral data showed signals due to olefinic protons as multiplate δ 5.4-5.3 (m, 4H, H-9, H-10, H-12, and H-13). The triplet signal at δ 2.7 (t, 2H, H-11) is due to the presence of allylic methylene protons. The intense multiplet peak at δ 1.2 (m, 10H) is due to the presence of many methylenes. The multiplet up-field proton signal at δ 0.9 (t, 3H) is evident for the presence of terminal methyl proton in the compound.

In the ^{13}C-NMR (Appendix 8), four sp^2 methines appeared at δ 130.2 (C-9), 130.0 (C-10), 128.0 (C-12), and 127.9 (C-13). In addition, peaks at δ 22.0-34.1 correspond to the methylene groups flanked between two Sp^2 methines at δ 34.1 (C-11). The terminal methyl group appeared at δ 14.0 (C-1 and C-21). The above spectral data suggest that the compound is 5, 12-henicosadiene (**31**). This is the first time 5, 12-henicosadiene (**31**) is isolated from *Scadoxus multiflorus,* and reported herein for first time from genus Scadoxus.

Table 6: ^{1}H and ^{13}C NMR spectral data of 5, 12-henicosadiene (**31**)

Position	δ_H(δ in ppm)	^{13}C NMR (δ_C in ppm)
C_1 & C_{21}	0.9 (t, 6H)	14.0
C_2 & C_{20}	1.3 (m, 4H)	29.9
C_3-C_7 & C_{15}–C_{19}	1.2 (m, 20H)	29.7
C_8	2.3 (m, 2H)	31.5
C_9	5.4 (m, 1H)	127.9
C_{10}	5.4 (m, 1H)	130.0
C_{11}	2.7 (t, 2H)	34.1
C_{12}	5.3 (m, 1H)	128.1
C_{13}	5.3 (m, 1H)	130.2
C_{14}	2.4 (m, 2H)	31.9

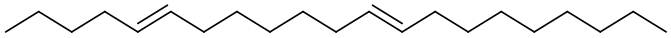

31

Figure 5: Structure of 5, 12-henicosadiene (**31**)

Lindcarpine derivatives (**32**) (36 mg) was isolated as a reddish brown with R_f value of 0.50 (70%EtOAc in *n*-hexane as eluent). The ^{1}H NMR (Appendix 12) spectral data revealed the existence of aromatic protons at δ 6.5 (s, 1H) and 6.14 (t, 2H). The corresponding signals of the olefinic protons with chemical shifts at δ 5.37 (dd, 1H) were also observed. The signal at δ 1.3 (m, 25H) is a characteristic signal for many methylene protons in the compound which was supported by the appearance of an intense carbon signal at δ 29 in the ^{13}C-NMR spectrum (Appendix 13). The signal observed at δ 2.8 (m, 2H) is ascribed to methylene protons attached to a carboxyl group. The signal at δ 2.6 (m, 4H) suggests allylic methylene. An up-field proton signal at 0.9 (m, 6H) is evident for the presence of terminal methyl proton in the compound.

The ^{13}C NMR spectrum with the aid of DEPT-135 (Appendix 2 and 3) revealed the existence of a carbonyl group (-CO-) at δ 204.4 attributed to ketone carbonyl. The carbon signal at δ 22- 34.1 corresponds to the methylene groups of which the most deshilded one that appeared at δ 34.1 suggests methylene next to a carbonyl. The most up-field carbon signal at δ 14.2 suggests the presence of terminal methyl groups. Three quaternary carbon appeared at δ 41.1, 41.0, and 40.5. Also, twelve sp^2 methines appeared at δ 145.5, 142.6, 137.2, 130.2, 130.0,

129.3, 128.9, 128.1, 127.9, and 127.0. From the above spectral data, the structure of the compound was identified as lindcarpine derivatives (**32**). This is the first time lindcarpine derivatives (**32**) were isolated from *Scadoxus multiflorus*, and it's new to the genus *Scadoxus*.

Table 7: ^{1}H and ^{13}C NMR spectral data of compound **32**

Position	δ_H(δ in ppm)	^{13}C NMR (δ_C in ppm)	DEPT-135 (δ_C in ppm)
1	-	142.5	-
2	-	145.5	-
3	-	126.9	-
1a	-	130.2	-
1b	-	129.3	-
1c	-	128.9	-
4	1.2 (2H)	29.0	29.0
5	2.05 (2H)	31.9	31.9
6	-	41.1	-
7	1.3 (2H)	29.7	29.7
8	-	128.1	-
9	6.5 (1H)	127.5	127.5
10	-	137.2	-
11	6.13 (1H)	127.9	127.9
12	6.14 (1H)	129.3	129.3
12a	-	127.0	-
13	2.18 (2H)	34.1	34.1
14	-	201.4	-
15	0.9 (3H)	22.5	22.5
16	1.4 (2H)	24.7	24.7
17	-	41.0	-
18	1.7 (2H)	22.6	22.6
19	0.9 (3H)	14.0	14.0
20	0.9 (3H)	14.1	14.1
21	1.6 (3H)	25.6	25.6
22	-	40.5	-
23	1.3 (2H)	22.5	22.5

24	0.9 (3H)	14.1	14.1
25	0.9 (3H)	13.9	13.9
26	1.4 (2H)	27.2	27.2
27	5.37 (1H)	130.0	130.0
28	-	130.2	-
29	1.2 (3H)	28.9	28.9
30	1.2 (3H)	22.6	22.6

\

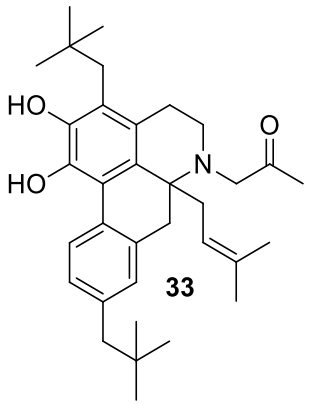

33

Figure 6: Structure of lindcarpine derivatives

Linolieamide (**33**) (30 mg) was isolated as a yellow solid with R_f value of 0.49 (70%EtOAc in hexane as eluent). The ^{1}H NMR (Appendix 12) spectral data showed the corresponding signals of the olefinic protons with chemical shifts between δ 5.57-5.30 (brs, 4H, H-9, H-10, H-12, and H-13). The multiplate signal at δ 1.3 (m, 16H) is a characteristic signal for many methylene protons in the compound which was supported by the appearance of an intense carbon signal at δ 29 in the ^{13}C-NMR spectrum (Appendix 13). The triplet signal observed at δ 2.14 (t, 2H, H-2) is ascribed to methylene protons attached to a carboxyl group. The triplet signal at δ 2.72 (t, 2H, H-11) suggests a proton that is flanked between two olefinic protons. The multiplate signal at δ 2.18 (m, 4H, H-8 & H-14) are integrated for the allylic methylene protons. The up-field triplet proton signal at δ 0.85 (t, 3H, H-18) is evident for the presence of terminal methyl proton in the compound.

The ^{13}C NMR spectral data with the aid of DEPT-135 (Appendix 13-14) revealed the existence of a carbonyl group (-CO-) at δ 175.0 (C-1) attributed to amide carbonyl. The carbon signal at δ 22-34.1 corresponds to the methylene groups of which the most deshilded

one that appeared at δ 34.1 suggests methylene next to carbonyl (C-2). The most up-field carbon signal at δ 14.2 (C-18) suggests the presence of terminal methyl groups. Also, four sp^2 methines appeared at δ 130.4 (C-10), 130.2 (C-13), 128.1 (C-9), and 127.5 (C-12). From the above spectral data and comparison with the literature, the structure of the compound was identified as linoleamide (**33**). Linoleamide is a fatty amide obtained from linoleic acid. Hanh *et al* (2011) report the isolation of linoleamide (**33**) from methanol extract of *Chromolaena odorata (*Asteraceae*)* aerial parts and examined their anti-inflammation proper. Linoleamide (**32**) inhibited the NO production at concentrations consistent with those required for NF-kB inhibition with IC_{50} values of 25.10 ±3.20 and 24.00 ±4.81 μM (Hanh *et al*., 2011). This is the first time linoleamide (**32**) isolated from *S. multiflorus* and reported herein for the first time from the genus.

Table 8: ^{1}H and ^{13}C NMR spectral data of linolieamide (**33**)

	linolieamide (**33**)		(Hanh *et al*., 2011)	
Position	δ_H(δ in ppm)	^{13}C NMR (δ_C in ppm)	δ_H(δ in ppm)	^{13}C NMR (δ_C in ppm)
1	-	175.0	-	174.9
2	2.2 (t, 2H)	34.1	2.2 (t)	34.0
3	1.5 (m, 2H)	24.9	1.5 (m)	24.8
4-6	1.2 (m, 6H)	29.1	1.2-1.4 (m)	29.0
7	1.3 (m, 2H)	28.9	1.2-1.4 (m)	28.9
8	2.1 (m, 2H)	27.0	2.0 (m)	27.1
9	5.4 (m, 1H)	128.1	5.36 (m)	128.1
10	5.4 (m, 1H)	130.4	5.36 (m)	130.2
11	2.6 (t, 2H)	29.5	2.76 (t)	29.5
12	5.3 (m, 1H)	127.5	5.36 (m)	128.1
13	5.3 (m, 1H)	130.2	5.36 (m)	130.2
14	1.5 (m, 2H)	31.3	1.5 (m)	29.2
15	1.2 (m, 2H)	27.0	1.2 (m)	27.6
16	1.2 (m, 2H)	31.4	1.2 (m)	31.5
17	1.2 (m, 2H)	22.5	1.2 (m)	22.5
18	0.8 (t, 3H)	14.2	0.8 (t)	14.0

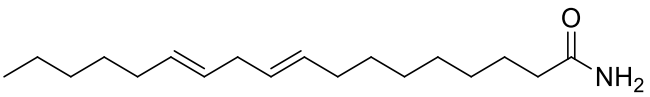

33

Figure 7: Structure of linoleamide

4.4 Anti-bacterial Activity

The crude extract and isolated compounds were tested for their antibacterial activity *in vitro* against *E. coli, P. aroginosa, K. pnimoniea, E. fecalis, S. thphimurium,* and *S. aureaus* at different concentrations (100, 50, 25, 12.5 mg/mL) for crude extract, and isolated compounds (10, 5, 2.5, 1.25 mg/mL). Ciprofloxacin as a positive control and DMSO as negative control were used. The mean zone of inhibition values indicated that all the compounds exhibited antibacterial activities ranging from 6.67 mm to 15.00 mm. Activity increased in a dose-dependent manner. All extract shows activity against *E. coli, K. pnimoniea, E. fecalis, and S. thphimurium.* The chloroform extract shows promising activity against *E.coli, E. fecalis, and S. aureaus* (12.67±0.58) as compared to ciprofloxacin (26.67±2.73, 23.50±1.38, and 28.00±1.67 respectively) as shown in **Table 9**. Hexane extract also shows promising activity against *E. fecalis* (15.00±0.0) and *S. aureaus* (14.00±1.0) as compared to ciprofloxacin (23.50±1.38, and 28.00±1.67 respectively). Methanol extract shows promising activity against *E.coli* and *E. fecalis* (12.00±0.00) compared to ciprofloxacin (26.67±2.73 and 23.50±1.38 respectively).

The zone of inhibition values indicated that all the compounds exhibited antibacterial activities ranging from 6.67-15 mm (**Table 10**) against all the tested bacterial strains except for *E. fecalis*. *β*-sitosterol (**29**) and 11-hentriacontene (**30**) showed promising activity (15.00±0.00) against *S. thphimurium* whereas 5, 12-henicosadiene (**31**) and *β*-sitosterol (**29**) showed promising activity (14.67±0.58 and 14±1.00) against *P. aroginosa* respectively as compared to ciprofloxacin (31.33±1.97 and 30.00±0.89 respectively). Linolieamide (**33**) and 11-hentriacontene (**30**) **also** showed promising activity (12.67±0.58 and 12.00±1.00) against *E.coli* respectively, whereas 5, 12-henicosadiene (**31**) and *β*-sitosterol (**29**) *β*-sitosterol (**29**) also showed promising activity (13.33±1.15 and 12.67±1.15) against *S. aureus* as compared to ciprofloxacin (26.67±2.73 and 28.00±1.67 respectively). Lindcarpine derivatives (**32**) and *β*-sitosterol (**29**) show promising activity against *K. pneumonia* (12.67±2.52 and 12.33 ±0.58)

respectively compared to ciprofloxacin (24.67±0.82). No inhibition zone was observed isolated compound against *E. fecalis.*

Table 9: Antibacterial activity of *S. multiflorus* root extract

Sample	Conc (mg/mL)	Inhibition Diameter (mm)±SD					
		E. coli	*P. aroginosa*	*K. pneumoniea*	*E. fecalis*	*S. thphimurium*	*S. aureaus*
Chloroform	100	12.67±0.58	NA	11.33±0.58	12.67±0.58	11.33±1.15	12.67±0.58
	50	12.33±0.58	NA	10.33±0.58	12.00±0.00	11.00±0.00	11.00±2.65
	25	11.33±0.58	NA	9.33±0.58	12.00±2.00	11.00±0.00	8.33±2.31
	12.5	11.33±0.58	NA	8.33±0.58	11.67±1.5	10.33±0.58	NA
Hexane	100	12.33±0.58	NA	11.67±0.58	15.00±0.0	13.00±1.73	14.00±1.0
	50	11.67±0.58	NA	11.00±1.0	13.00±1.0	11.67±1.53	13.00±1.0
	25	11.00±1.00	NA	10.33±0.58	13.00±1.0	9.00±1.5	12.33±1.0
	12.5	10.33±0.58	NA	NA	11.00±1.0	7.67±2.0	12.00±0.0
Methanol	100	12.00±0.00	NA	9.00±1.00	12.00±0.00	11.00±0.00	NA
	50	10.33±0.58	NA	8.00±0.00	NA	10.00±0.00	NA
	25	9.00±1.00	NA	7.00±0.58	NA	NA	NA
	12.5	NA	NA	7.00±0.00	NA	NA	NA
Ciprofloxacin (µg/mL)	10	26.67±2.73	30.00±0.89	24.67±0.82	23.50±1.38	31.33±1.97	28.00±1.67

Table 10: Antibacterial activity of isolated compounds

Sample	Conc (mg/mL)	Inhibition Diameter (mm)±SD					
		E. coli	*P. aroginosa*	*K. pneumoniea*	*E. fecalis*	*S. typhimurium*	*S. aureus*
β-sitosterol (**29**)	10	10.67±1.5	14.00±1.00	12.33±0.58	NA	15.00±0.00	12.67±1.15
	5	10.00±1.73	13.67±0.58	11.67±1.15	NA	14.00±2.00	12.33±1.15
	2.5	8.33±2.52	12.00±1.00	11.33±1.53	NA	11.33±0.58	12.00±.00
	1.25	7.67±2.89	10.67±0.58	10.33±0.58	NA	11.00±0.00	9.33±2.08
11-	10	12.00±1.00	12.67±2.08	9.67±2.31	NA	12.33±0.58	12.33±0.58

hentriacontene (**30**)	5	11.67±0.58	11.00±0.00	9.33±2.08	NA	11.67±0.58	12.00±1.00
	2.5	11.00±0.00	11.00±.00.00	9.00±1.73	NA	11.00±1.00	11.67±1.53
	1.25	10.67±0.58	11.00±0.00	8.67±1.53	NA	10.33±0.58	11.00±1.00
5, 12-henicosadiene (**31**)	10	11.33±1.15	13.00±1.00	8.00±0.00	NA	15.00±0.00	13.33±1.15
	5	10.67±0.58	11.00±0.00	7.00±0.00	NA	13.33±0.58	13.33±1.53
	2.5	10.67±0.58	10.33±0.58	6.67±0.58	NA	12.67±1.53	12.00±1.00
	1.25	10.00±0.00	7.67±0.58	NA	NA	11.33±1.15	9.67±2.52
Lindcarpine derivatives (**32**)	10	11.67±1.15	14.67±0.58	12.67±2.52	NA	13.00±2.00	13.00±1.00
	5	10.00±1.00	12.33±2.31	9.67±2.52	NA	12.33±0.58	13.00±1.00
	2.5	9.67±1.53	12.33±2.31	8.33±2.31	NA	12.00±1.00	12.33±1.53
	1.25	9.00±1.00	10.33±0.58	8.00±1.73	NA	11.33±0.58	11.33±1.53
Linolieamide (**33**)	10	12.67±0.58	13.00±1.00	9.67±1.53	NA	13.33±1.54	12.33±0.58
	5	11.67±0.58	12.00±0.00	8.00±2.00	NA	13.00±1.00	12.33±0.58
	2.5	11.33±0.58	12.00±0.00	8.00±2.00	NA	11.00±1.00	12.33±0.58
	1.25	10.33±0.58	11.00±0.00	NA	NA	10.67±0.58	11.33±1.15
Ciprofloxacin (µg/mL)	10	26.67±2.73	30.00±0.89	24.67±0.82	23.50±1.38	31.33±1.97	28.00±1.67

NA = No Activity, SD = Standard Deviation, mean values of three triplicates ± standard deviation

4.5 Antioxidant Activity

The DPPH scavenging assay, crude extracts, and isolated compounds of *S. multiflorus* were investigated for their free radical scavenging activity via their reaction with the stable DPPH radicals. The reduction of the DPPH was followed by a decrease in absorbance at 517 nm. The DPPH radical scavenging activities (%) of extracts and isolated compounds were found to be 68.80 (methanol extract), 41.3 (chloroform extract), 31.3 (linolieamide (**33**), 25.39 (*β*-sitosterol (**29**)**,** 21.38 (5, 12-henicosadiene (**31**), 21.29 (lindcarpine derivatives (**32**) and 21.20 (11-hentriacontene (30), 10.79 (hexane crude) respectively at 200 µg/mL and 20 µg/mL (**Table 11** and **12**). It was observed that the DPPH scavenging activity increased with the increasing concentration of the samples in the assay. For the various concentrations, compound **33** exhibited the highest percent inhibition of the DPPH as compared to the other isolated compounds. The positive control, ascorbic acid showed maximum scavenging effect at very low and high concentrations (96.11, 95.63, 95.43, and 95.14 % at 200, 100, 50, and 25

µg/mL) for extract and (97.36, 96.72, 92.27 and 87.35 % at 20, 10, 5, and 2.5 µg/mL) for isolated compounds (**Figure 11** and **12**). When compared to standard ascorbic acid, the DPPH radical scavenging activity of *S. multiflorus* extracts and isolated compounds were lower.

Table 11: DPPH radical scavenging activities (%) of *S. multiflorus* root extract

Conc (µg/mL)	Control	Extracts						Positive control	
		Hexane		Chloroform		Methanol		Ascorbic Acid	
		A	%RSA	A	%RSA	A	%RSA	A	%RSA
200	1.029	0.918	10.79	0.604	41.3	0.321	68.80	0.04	96.11
100	1.029	0.919	10.69	0.644	37.41	0.634	38.39	0.045	95.63
50	1.029	0.935	9.14	0.781	25.27	0.76	26.14	0.047	95.43
25	1.029	0.965	6.22	0.769	24.1	0.862	16.23	0.05	95.14
IC_{50}		409.1		344.9		393.9		0.0007	

Table 12: DPPH radical scavenging activities (%) of isolated compounds

Conc (µg/mL)	Control	Compounds					
		β-sitosterol (**29**)		11-hentriacontene (**30**)		5, 12-henicosadiene (**31**)	
		A	%RSA	A	%RSA	A	%RSA
20	1.099	0.82	25.38672	0.864	21.20109	0.864	21.38308
10	1.099	0.872	20.65514	0.885	20.56415	0.885	19.47225
5	1.099	0.875	20.38217	0.887	20.20018	0.887	19.29026
2.5	1.099	0.89	19.01729	0.902	19.10828	0.902	17.92539
IC_{50}		64.5		169.6		121.5	
Conc (µg/mL)	Control	Compound				Positive control	
		lindcarpine derivatives (**32**)		linolieamide (**33**)		Ascorbic Acid	
		A	%RSA	A	%RSA	A	%RSA
20	1.099	0.865	21.29208	0.865	31.30118	0.029	97.36124
10	1.099	0.88	19.92721	0.88	23.47589	0.036	96.72429
5	1.099	0.887	19.29026	0.887	19.92721	0.085	92.2657

2.5	1.099	0.907	17.47043	0.907	14.83167	0.139	87.35214
IC_{50}		111.9		64.4		4	

Conc-Concentration, A- Absorbance, RSA-Radical Scavenging Activity

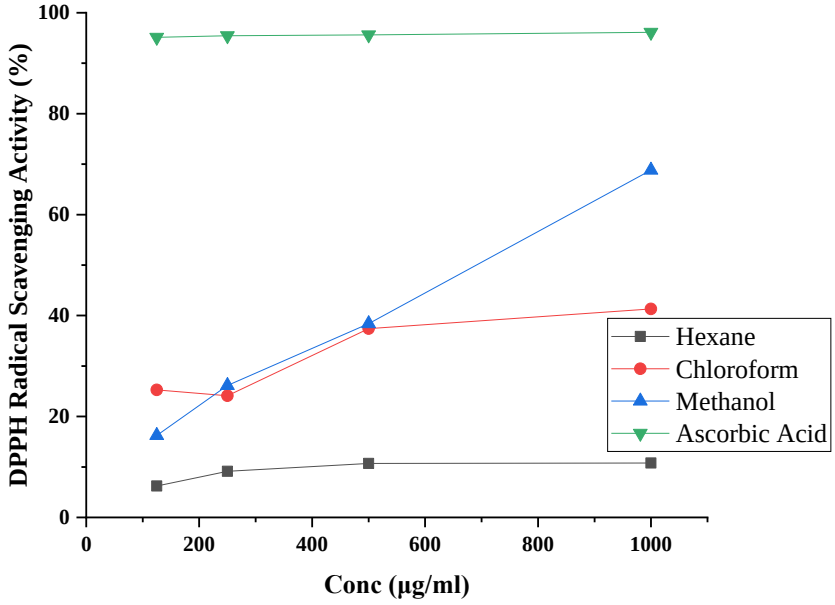

Figure 8: DPPH radical scavenging activities (%) of *S. multiflorus* root extract

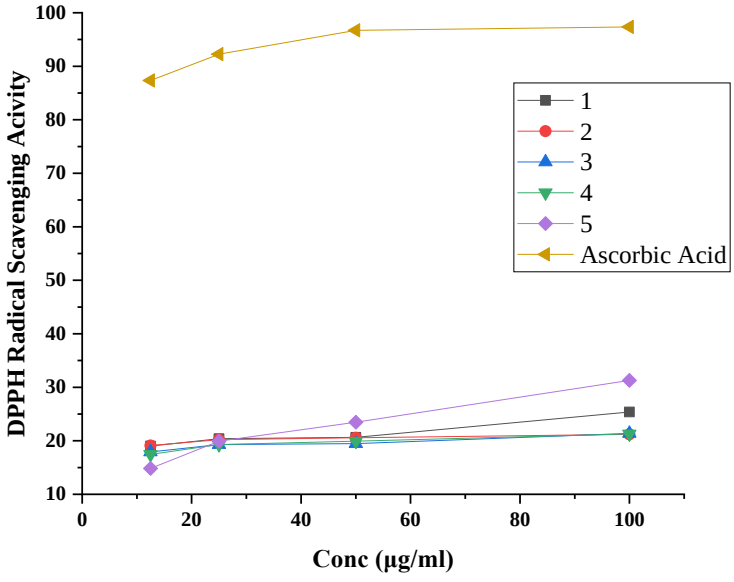

Figure 9: DPPH radical scavenging activities (%) of isolated compounds

4.6 *In silico* molecular Docking Study

4.6.1 *In silico* molecular Docking Study of (*E.coli*) enzyme DNA gyrase

In silico study of isolated compounds inhibitors as antibacterial drug candidates were conducted to predict the orientation and binding affinity at the active site of the receptor. In this regard, the molecular docking analysis for the isolated compounds was performed to elucidate their binding interactions with bacterial (*E.coli*) enzyme DNA gyrase. The binding affinity, H-bond, and residual interaction of the isolated compounds and Amoxicillin are summarized in **Table 13**. In the docking study, all the compounds were found to have minimum binding energy ranging from − 5.4 to − 9.1 kcal/mol. From these, the best result was achieved by *β*-sitosterol (**29)** (− 9.1 kcal/mol) compared with standard Amoxicillin (-7.6). 11-hentriacontene (**30**) showed minimum binding energy of − 5.4 whereas 5, 12-henicosadiene (**31**)**,** lindcarpine derivatives (**32**)**,** and linolieamide (**33**) showed better activity of − 5.9, − 7.3, and − 5.9 kcal/mol respectively.

All the compounds except 11-hentriacontene (**30**) and 5, 12-henicosadiene (**31**) have shown hydrogen bonding interaction. *β*-sitosterol (**29)** showed H-bonding interaction with amino acid Ser-1084, lindcarpine derivatives (**32**) showed interaction with Arg-76, Arg-76, and Gly-101, Gly-117, and linolieamide (**33**) showed interaction Val-167, Val-71, Thr-165, and Asp-73 as shown in **Table 13** below. All compounds exhibited more residual Van der Waals interaction than the standard drug ciprofloxacin.

Table 13: Molecular docking results of isolated compounds against *E. coli* Gyrase B (PDB ID 7P2W)

Compounds	Affinity (kcal/mol	H-bond	Residual interactions	
			Hydrophobic and Electrostatic	Van der Waals
β-sitosterol (**29)**	− 9.1	Asp-73	Hydrophobic Alkyl- Ile-78, Ile-94	Gly-117, Val-118, Arg-76, Glu-50, Gly-77, Thr-165, Asn-46, Asp-49, Gly-101
11-hentriaconte	− 5.4	-	Hydrophobic Alkyl- Ala-47, Pro-79, Ala-90, Ala-100, Val-120, Val-93, Val-43, Val-71, Ile-78 (Dist. 5.09637 Å), Ile-78	Glu-50, Asn-46, Val-167, Thr-165, Asp-73, Gly-77, Arg-76, Gly-101

ne (**30**)			(Dist. 5.04935 Å), Ile-78 (Dist. 4.86398 Å), Ile-78 (Dist. 5.44283 Å), Val-118 (Dist. 5.30437 Å), Val-118 (Dist. 4.42964 Å), Val-118 (Dist. 5.45992 Å), Ile-94 (Dist. 5.12032 Å), Ile-94 (Dist. 5.47553 Å), Ile-94 (Dist. 4.72673 Å) Hydrophobic-Pi-Alkyl- His-83 (Dist. 5.08018 Å), His-83 (Dist. 4.35868 Å)	
5, 12-henicosadiene (**31**)	− 5.9	-	Hydrophobic Alkyl- Pro-79, Ala-90, Ala-100, Val-120, Val-93, Ile-78 (Dist. 3.99016 Å), Ile-78 (Dist. 5.07864 Å), Ile-78 (Dist. 5.39231 Å), Ile-78 (Dist. 5.07899 Å), Val-118 (Dist. 3.65658 Å), Val-118 (Dist. 5.17594 Å), Ile-94 (Dist. 4.5859 Å), Ile-94 (Dist. 5.05691 Å), Ile-94 (Dist. 4.4657 Å) Hydrophobic-Pi-Alkyl- His-83 (Dist. 5.07955 Å), His-83 (Dist. 4.68723 Å)	Thr-165, Asp-73, Ala-47, Asn-46, Glu-50
lindcarpine derivatives (**32**)	− 7.3	Arg-76 (Dist. 2.06088 Å), Arg-76 (Dist. 3.06776 Å), Gly-101, Gly-117	Hydrophobic-Pi-Sigma-UNK1:C Hydrophobic Alkyl- Ala-90, Pro-79 (Dist. 4.63772 Å), Pro-79 (Dist. 4.50208 Å) Hydrophobic-Pi-Alkyl- Val-118	Gly-102, Ile-94, His-116, Asp-49, Ala-53, Ile-78, Glu-50, His-83, Gly-77
linoliamide (**33**)	− 5.9	Val-167, Val-71, Thr-165, Asp-73	Hydrophobic Alkyl- Ala-53, Ile-78 (Dist. 5.05266 Å), Ile-78 (Dist. 5.44767 Å), Val-118 (Dist. 5.0611 Å), Val-118 (Dist. 5.28247 Å) Hydrophobic-Pi-Alkyl- His-116	Asn-46, Glu-50, Arg-76, Gly-117, Ala-47, Asp-49, Gln-72, Met-166, Val-43, Val-120

Amoxicillin	− 7.6	Arg-76 (Dist. 2.45587 Å), Arg-76 (Dist. 2.49995 Å), Glu-50 (Dist. 3.03222 Å), Glu-50 (Dist. 3.13828 Å), Asn-46	Hydrophobic-Pi-Sigma- Ile-78 Hydrophobic-Amide-Pi-Stacked- A:Asn 46:C,O; Ala 47:N Hydrophobic-Pi-Alkyl- Val-118, Val-120	His-116, Gly-117, Asp-73, Asp-49, Thr-165, Val-43, Val-167, Leu-52, Ala-53, His-55, Pro-79

DA = deoxyadenosine; DG = deoxyguanosine; DT = deoxythymidine; DC =Deoxycytidine.

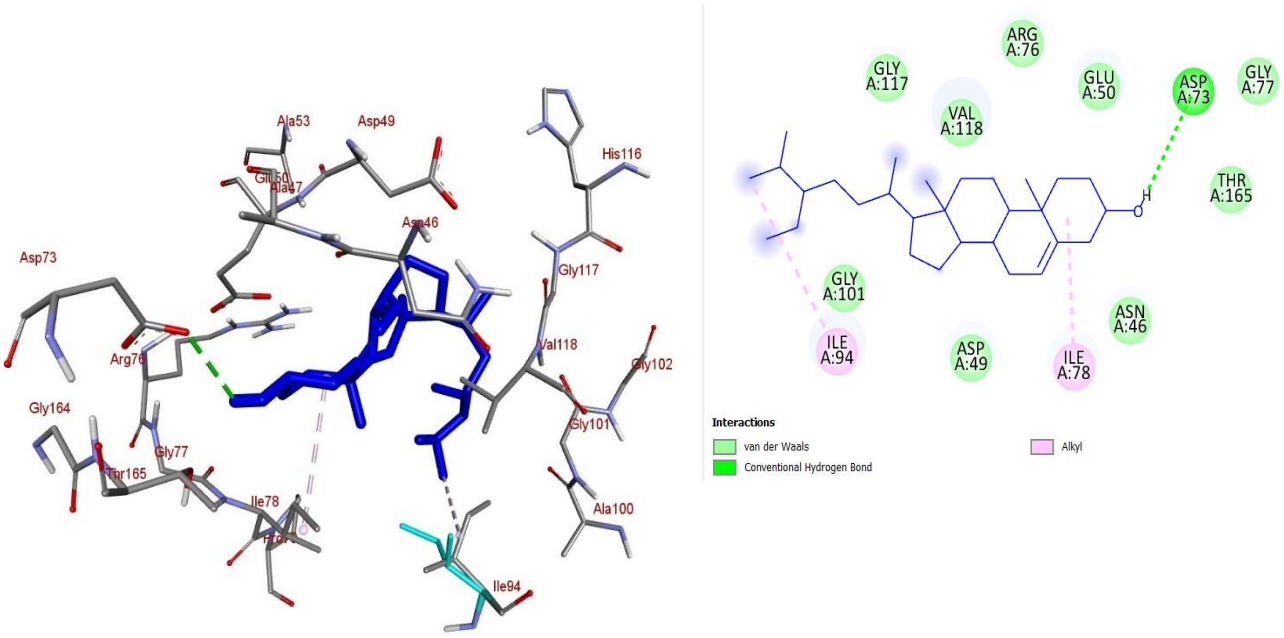

Figure 10: The 2D and 3D binding interactions of *β* –sitosterol **(29)** against *E. coli* Gyrase B (PDB ID: 7P2W).

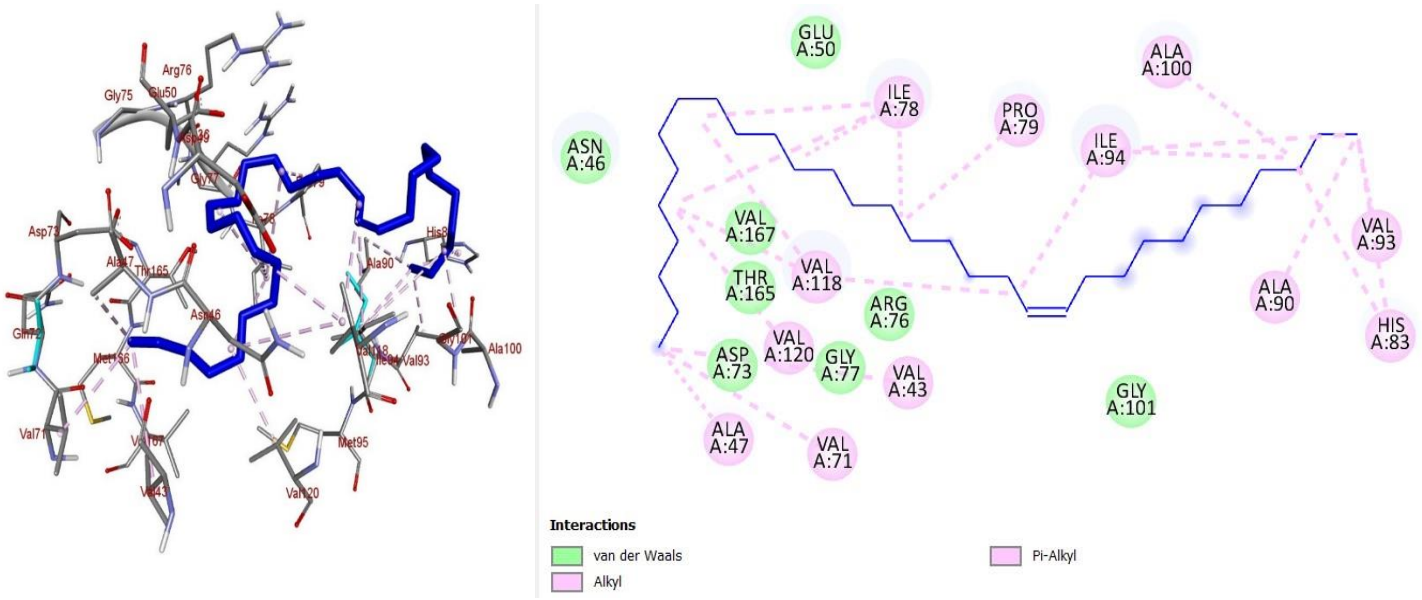

Figure 11: The 2D and 3D binding interactions of 11-hentriacontene (**30**) against *E. coli* Gyrase B (PDB ID: 7P2W).

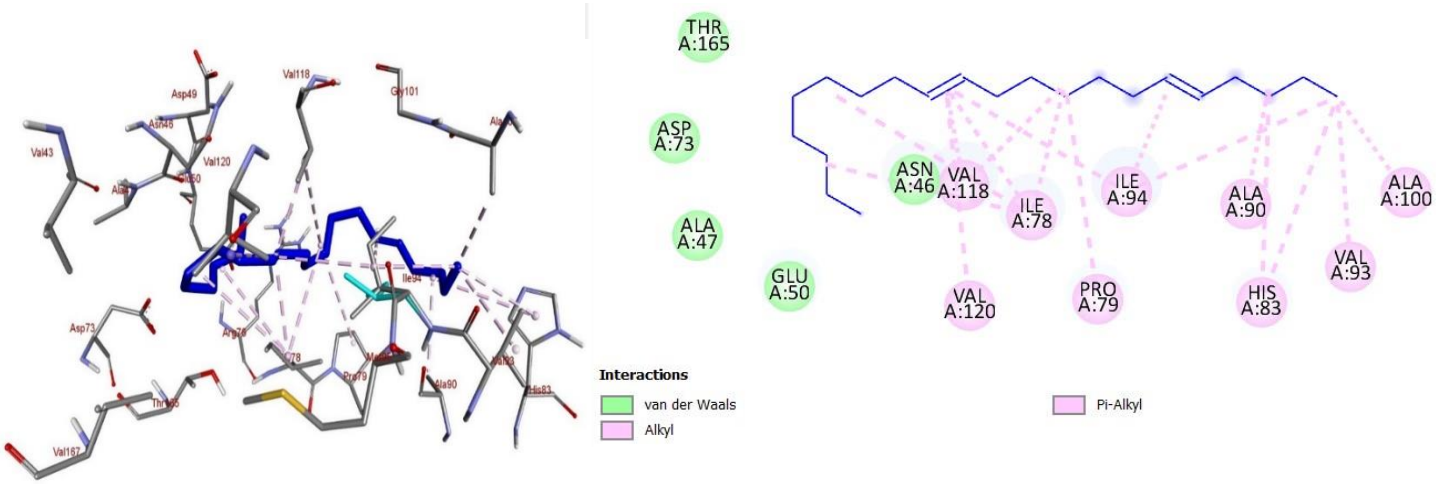

Figure 12: The 2D and 3D binding interactions of 5, 12-henicosadiene (**31**) against *E. coli* Gyrase B (PDB ID: 7P2W).

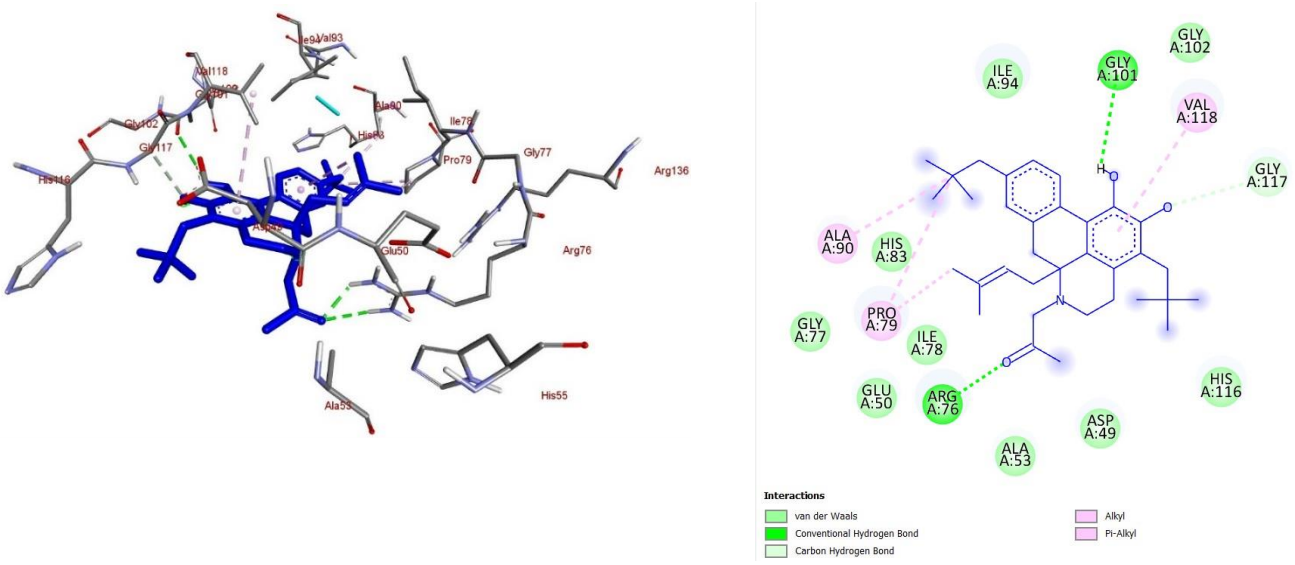

Figure 13: The 2D and 3D binding interactions of lindcarpine derivatives **(32)** against *E. coli* Gyrase B (PDB ID: 7P2W).

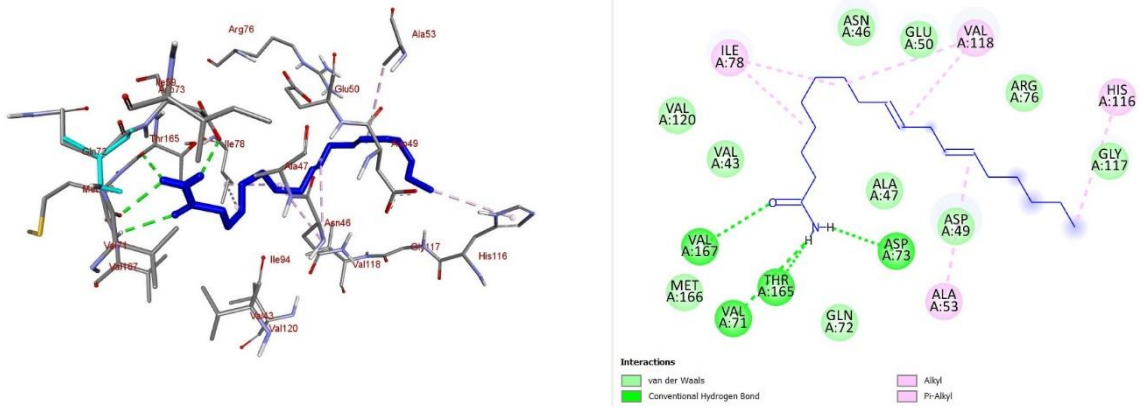

Figure 14: The 2D and 3D binding interactions of linolieamide **(33)** against *E. coli* Gyrase B (PDB ID: 7P2W).

4.6.2 *In silico* Molecular Docking Study of *S. aureus* Pyruvate Kinase

In silico study of isolated compounds inhibitors as antibacterial drug candidates were conducted to predict the orientation and binding affinity at the active site of the receptor. In this regard, the molecular docking analysis for the isolated compounds was performed to elucidate their binding interactions with bacterial *S. aureus* Pyruvate Kinase. The binding affinity, H-bond, and residual interaction of the isolated compounds and Amoxicillin are summarized in **Table 14**. In the docking study, all the compounds were found to have minimum binding energy ranging from − 5.2 to – 7.3 kcal/mol. From these, the best result

was achieved by lindcarpine derivatives (**32**) (− 7.3 kcal/mol) compared with standard c Amoxicillin (− 7.6 kcal/mol). 11-hentriacontene (**30**) showed minimum binding energy of − 5.2 whereas *β*-sitosterol (**29**), linolieamide (**33**) and 5, 12-henicosadiene (**31**) showed better activity of − 6.7, − 5.9, and − 5.5kcal/mol respectively.

All the compounds except 11-hentriacontene (**30**) and 5, 12-henicosadiene (**31**) have shown hydrogen bonding interaction. *β*-sitosterol (**29)** showed H-bonding interaction with amino acid Asp-237, lindcarpine derivatives (**32**) showed interaction with Gly-481, Ala-572, and linolieamide (**33**) showed interaction Arg-264, and Tyr-302 as shown in **Table 14** below. All compounds exhibited more residual Van der Waals interaction.

Table 14: Molecular docking results of isolated compounds against *S. aureus* Pyruvate Kinase (PDB ID 3T05)

Compounds	Affinity (kcal/mol	H-bond	Residual interactions	
			Hydrophobic and Electrostatic	Van der Waals
β-sitosterol (**29**)	− 6.7	Asp-237	Hydrophobic Alkyl- Val-356, Ala-573	Ser-354, Asn-357, Lys-390, Leu-269, Gln-574, Thr-463, Gly-462, Thr-464, Arg-484, Ser-383, Thr-387, Arg-386, Lys-271
11-hentriacontene (**30**)	− 5.2	-	Hydrophobic Alkyl- Ala-573 (Dist. 4.3573 Å), Ala-573 (Dist. 3.7971 Å), Leu-269 (Dist. 4.73456 Å), Leu-269 (Dist. 5.34504 Å), Leu-355 (Dist. 4.54528 Å), Leu-355 (Dist. 4.67746 Å), Val-356 (Dist. 5.01491 Å), Val-356 (Dist. 3.68814 Å), Val-356 (Dist. 5.47431 Å), Leu-471 (Dist. 4.32877 Å), Leu-471 (Dist. 4.83822 Å) Hydrophobic-Pi-Alkyl- Phe-578	Arg-484, Ser-354, Thr-387, Asn-357, Lys-390, Glu-352, Lys-268, Lys-271, Gln-574, Thr-463, Lys-576, His-470, Leu-449, Asp-571, Asn-583
5, 12-	− 5.5	-	Hydrophobic-Pi-Sigma- His-	Val-456, Gly-473, Glu-475,

henicosadiene (**31**)			470 Hydrophobic Alkyl- Leu-355 (Dist. 4.36508 Å), Leu-355 (Dist. 4.25559 Å), Leu-471 (Dist. 4.87423 Å), Leu-471 (Dist. 4.58438 Å), Leu-471 (Dist. 5.42126 Å), Lys-576, Pro-457 Hydrophobic-Pi-Alkyl- Phe-578 (Dist. 5.00889 Å), Phe-578 (Dist. 5.01208 Å)	Asp-474, Gln-574, Asp-571, Thr-463, Leu-449, Glu-460, Ile-469, Asn-465, Thr-461, Lys-468
Lindcarpine derivatives (**32**)	− 7.3	Gly-481, Ala-572 (Dist. 2.01283 Å), Ala-572 (Dist. 2.69651 Å)	Hydrophobic-Pi-Sigma-UNK1:C Hydrophobic-Pi-Alkyl- Ala-573	Ile-482, Gln-480, Gly-575, Gly-483, Glu-234, Arg-484, Lys-271, Val-356, Gln-574, Lys-576, Gly-479, Asn-478, Ser-381, Gly-462, Ser-383, Thr-463
Linolieamide (**33**)	− 5.9	Arg-264 (Dist. 2.10006 Å), Arg-264 (Dist. 2.55986 Å), Tyr-302	Hydrophobic Alkyl- Lys-260 (Dist. 5.32285 Å), Lys-260 (Dist. 4.27123 Å), Arg-264, Met-257 Hydrophobic-Pi-Alkyl- Tyr-302 (Dist. 4.43028 Å), Tyr-302 (Dist. 5.31670 Å)	Asp-303, Asp-261, Ala-337, Gln-338, Asp-339, Arg-347, Leu-343, Lys-342, Lys-260
Amoxicillin	− 7.6	Arg-76 (Dist. 2.45587 Å), Arg-76 (Dist. 2.49995 Å), Glu-50 (Dist. 3.03222 Å), Glu-50 (Dist. 3.13828 Å), Asn-46	Hydrophobic-Pi-Sigma- Ile-78 Hydrophobic-Amide-Pi-Stacked- A:Asn 46:C,O; Ala 47:N Hydrophobic-Pi-Alkyl- Val-118, Val-120	His-116, Gly-117, Asp-73, Asp-49, Thr-165, Val-43, Val-167, Leu-52, Ala-53, His-55, Pro-79

DA = deoxyadenosine; DG = deoxyguanosine; DT = deoxythymidine; DC =Deoxycytidine.

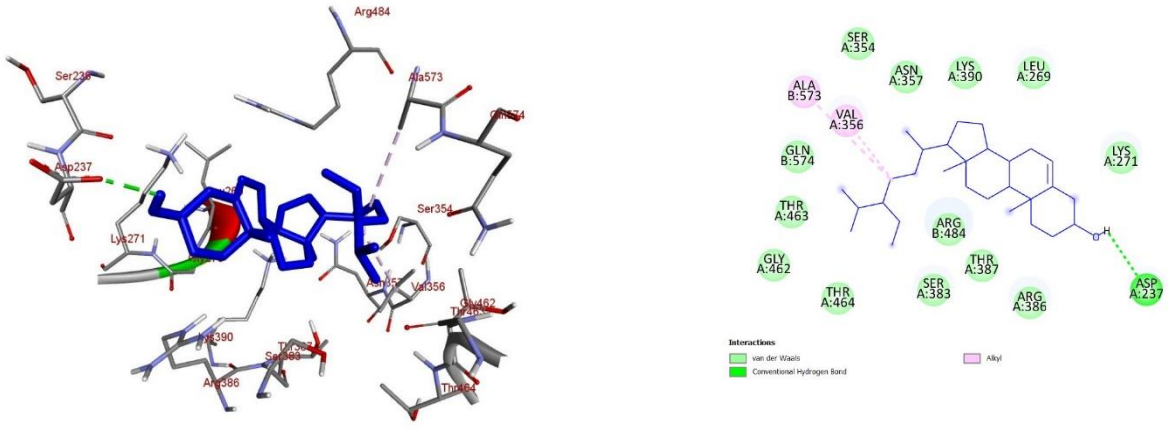

Figure 15: The 2D and 3D binding interactions of *β*-sitosterol **(29**) against *S. aureus* Pyruvate Kinase (PDB ID 3T05).

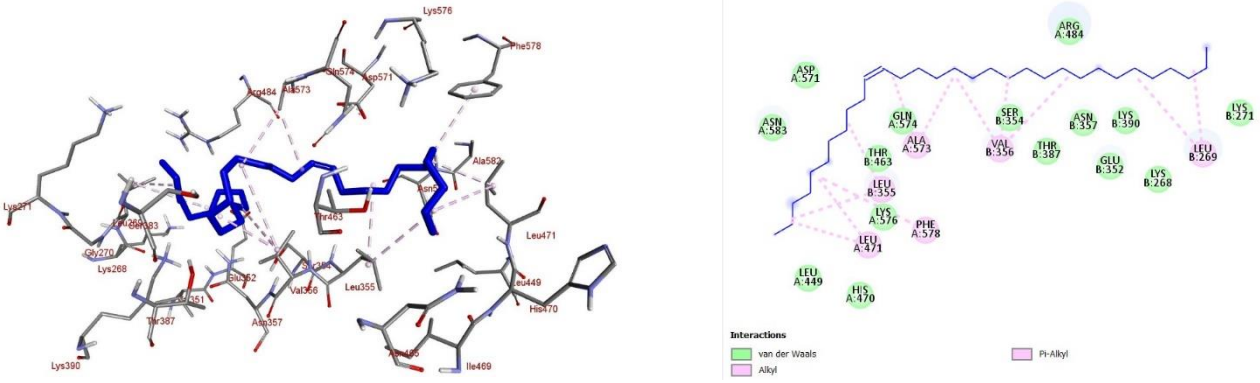

Figure 16: The 2D and 3D binding interactions of 11-hentriacontene **(30)** against *S. aureus* Pyruvate Kinase (PDB ID 3T05).

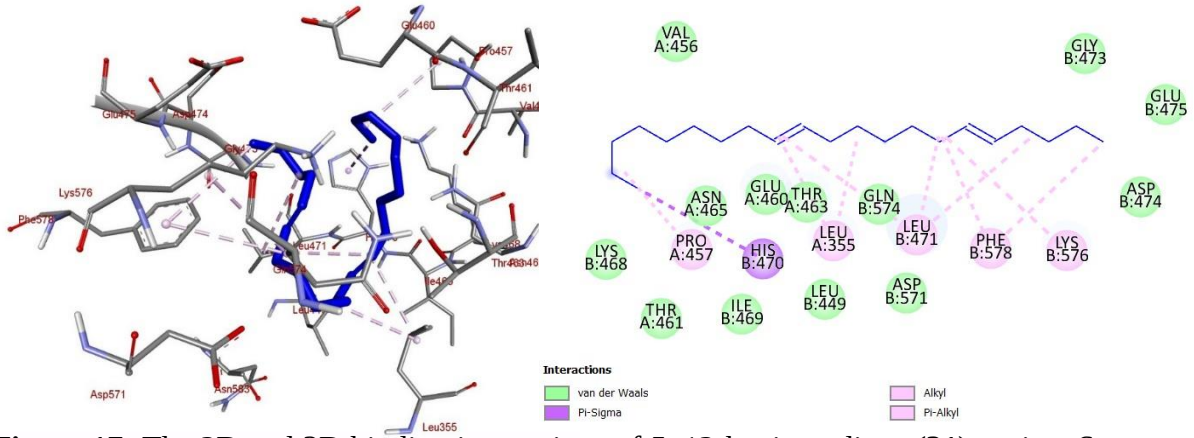

Figure 17: The 2D and 3D binding interactions of 5, 12-henicosadiene **(31**) against *S. aureus* Pyruvate Kinase (PDB ID 3T05).

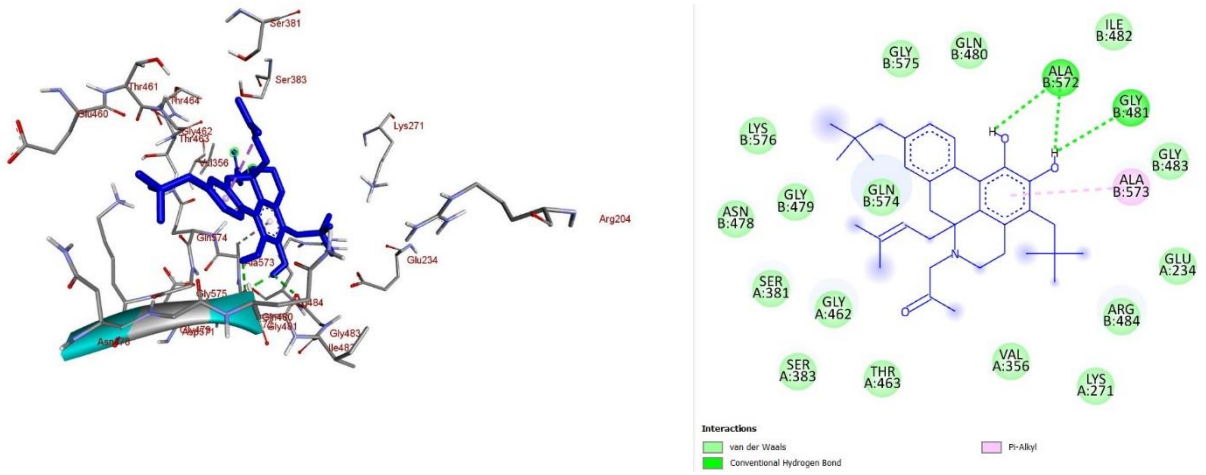

Figure 18: The 2D and 3D binding interactions of lindcarpine derivatives **(32)**, against *S. aureus* Pyruvate Kinase (PDB ID 3T05).

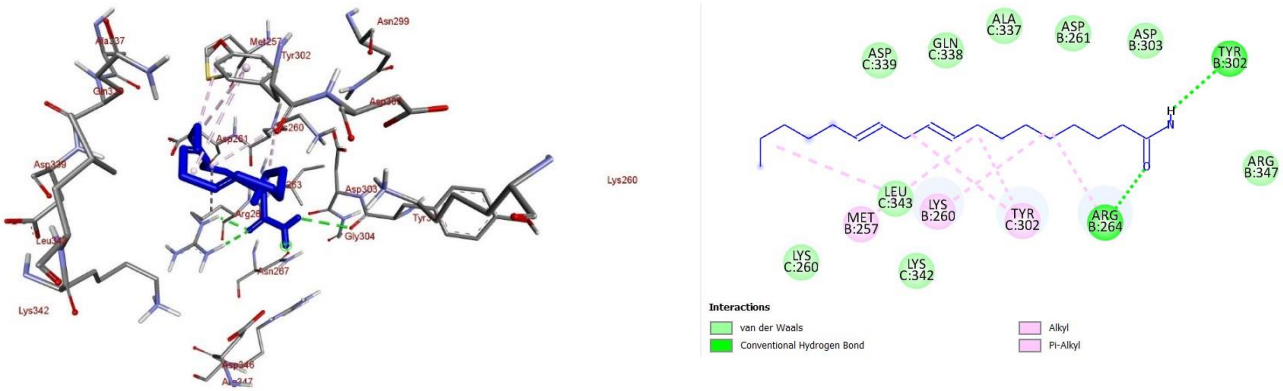

Figure 19: The 2D and 3D binding interactions of linolieamide **(33)** against *S. aureus* Pyruvate Kinase (PDB ID 3T05).

4.6.3 *In silico* Molecular Docking Study of topoisomerase II *β*

In silico study of isolated compounds inhibitors as anticancer drug candidates were conducted to predict the orientation and binding affinity at the active site of the receptor. In this regard, the molecular docking analysis for the isolated compounds was performed to elucidate their binding interactions with topoisomerase II *β*. The binding affinity, H-bond, and residual interaction of the isolated compounds and Abiraterone are summarized in **Table 14**. In the docking study, all the compounds were found to have minimum binding energy ranging from −6.3 to −9.6 kcal/mol. From these, the best result was achieved using *β*-sitosterol (**29**) (-9.6 kcal/mol) compared with standard Abiraterone (−11.8 kcal/mol). 5, 12-henicosadiene (**31**) showed minimum binding energy of -6.3 whereas compounds lindcarpine derivatives (**32**),

linolieamide (**33),** and 11-hentriacontene (**30**) showed better activity of −8.2, −6.6, and −6.5 kcal/mol respectively.

All the compounds except 11-hentriacontene (**30**) and 5, 12-henicosadiene (**31**) have shown hydrogen bonding interaction. *β*-sitosterol (**29)** showed H-bonding interaction with amino acid Met-782, lindcarpine derivatives (**32**) showed interaction with DC-16, DG-5, and DC-3 and linolieamide (**33**) showed interaction with Lys-456, DG-10, and DT-9 as showed in Table 14 below. All compounds exhibited more residual Van der Waals interaction than the standard drug Abiraterone.

Table 15: Molecular docking results of isolated compounds against Human topoisomerase II *β* (PDB ID 3QX3)

Compound	Binding Affinity (kcal/mol	H-bond	Residual interactions	
			Hydrophobic and Electrostatic	Van der Waals
β-sitosterol (**29)**	− 9.6	Met-782	Hydrophobic-Pi-Sigma- DC-8, DT-9 Hydrophobic-Alkyl- Arg-503 Hydrophobic-Pi-Alkyl- DC-8, DT-9, DG-13)	Gln-778, DA-12, Asp-479, Ser-480, Gly-478, Glu-477, DG-10, Gly-504
11-hentriacontene (**30**)	− 6.5	-	Hydrophobic-Pi-Sigma- DA-12 (Dist. 3.93063 Å), DA-12 (Dist. 3.82873 Å) Hydrophobic-Alkyl- Arg-503 (Dist. 4.73402 Å), Arg-503 (Dist. 3.82873 Å), Pro-819 Hydrophobic-Pi-Alkyl- DT-9 (Dist. 4.92104 Å), DT-9 (Dist. 4.9560 Å), DA-12 (Dist. 3.94588 Å), DA-12 (Dist. 4.68808 Å), DG-13 (Dist. 4.06784 Å), DG-13 (Dist. 4.54166 Å), DG-13 (Dist. 4.11522 Å), DC-8 (Dist. 4.51383 Å), DC-8 (Dist.	Met-782, Ser-818, Arg-820, DC-11, Gln-778, Gly-478, Gly-504, Asp-479, DG-10

			4.51380 Å)	
5, 12-henicosadiene (**31**)	− 6.3	-	Hydrophobic-Pi-Sigma- DG-13 Hydrophobic-Alkyl- Arg-503 (Dist. 5.0794 Å), Arg-503 (Dist. 3.85866 Å), Arg-503 (Dist. 5.0546 Å), Met-782 Hydrophobic-Pi-Alkyl- DT-9 (Dist. 4.31981 Å), DT-9 (Dist. 4.74874 Å), DA-12 (Dist. 5.32599 Å), DA-12 (Dist. 4.59638 Å), DC-8 (Dist. 3.96316 Å), DC-8 (Dist. 5.14848 Å), DG-13	Gln-778, Gly-478, Asp-479, DG-10
lindcarpine derivatives (**32**)	**− 8.2**	DC-16 (Dist. 2.48655 Å), DC-16 (Dist. 2.73075 Å), DG-5, DC-3	Electrostatic-Pi-Anion- DC-3 Hydrophobic Alkyl- Lys-814 Hydrophobic-Pi-Alkyl- DG-13	DA-6, Met-782, DA-12, DT-15, DC-14, DG-2
linolieamide (**33**)	**− 6.6**	Lys-456 (Dist. 2.36538 Å), Lys-456 (Dist. 2.47189 Å), DG-	Hydrophobic-Pi-Sigma- DA-12 Hydrophobic-Alkyl- Arg-503 (Dist. 4.67013 Å), Arg-503 (Dist. 3.87238 Å) Hydrophobic-Pi-Alkyl- DT-9 (Dist. 5.41136 Å), DT-9 (Dist. 4.12649 Å), DT-9 (Dist. 4.91044 Å), DA-12 (Dist. 4.64148 Å), DA-12 (Dist. 5.49342 Å), DG-13 (Dist. 5.33662 Å), DG-13 (Dist. 5.31801 Å), DG-13 (Dist. 5.48630 Å), DC-8	Asp-479, Gln-778

		10, DT-9		
Abiraterone	− 11.8	DG-10	Hydrophobic-Alkyl- Arg-503(Dist. 4.50057 Å) Hydrophobic-Alkyl- Arg-503(Dist. 4.19301 Å) Hydrophobic-Pi-Alkyl- DA-12 Hydrophobic-Pi-Alkyl- DC-8	Gly-504, Glu-477, Gly-478, Lys-456, Asp-479, DT-9

DA = deoxyadenosine; DG = deoxyguanosine; DT = deoxythymidine; DC = Deoxycytidine

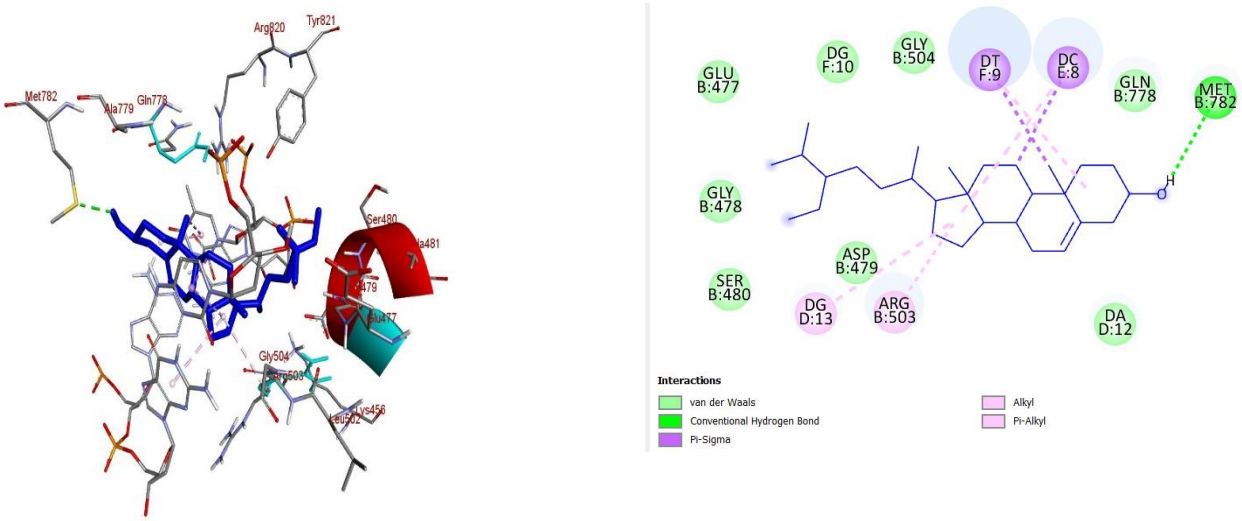

Figure 20: The 2D and 3D binding interactions of *β*-sitosterol (29) against human topoisomerase II*β* (PDB ID: 3QX3).

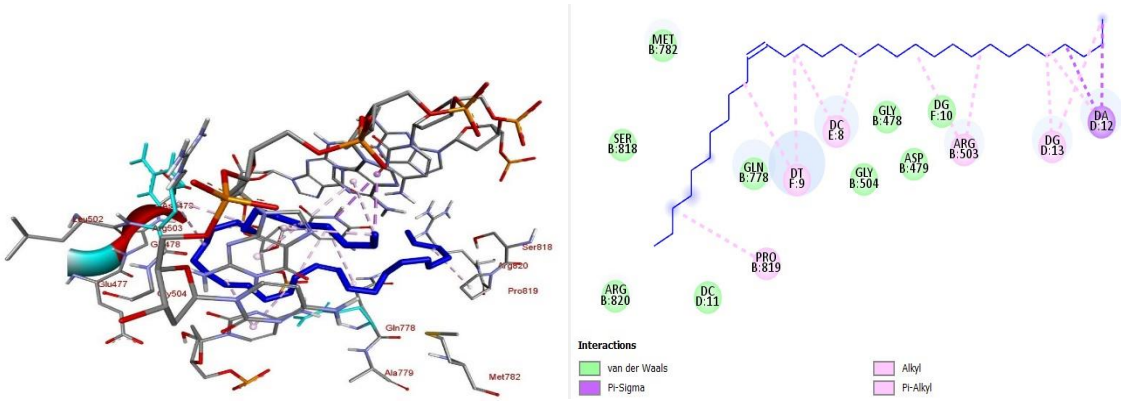

Figure 21: The 2D and 3D binding interactions of 11-hentriacontene **(30)** against human topoisomerase II*β* (PDB ID: 3QX3).

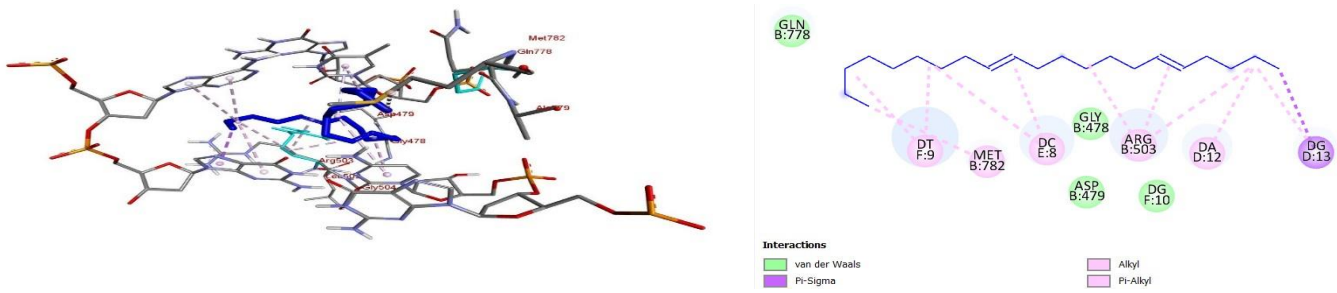

Figure 22: The 2D and 3D binding interactions of 5, 12-henicosadiene **(31)** against human topoisomerase II*β* (PDB ID: 3QX3).

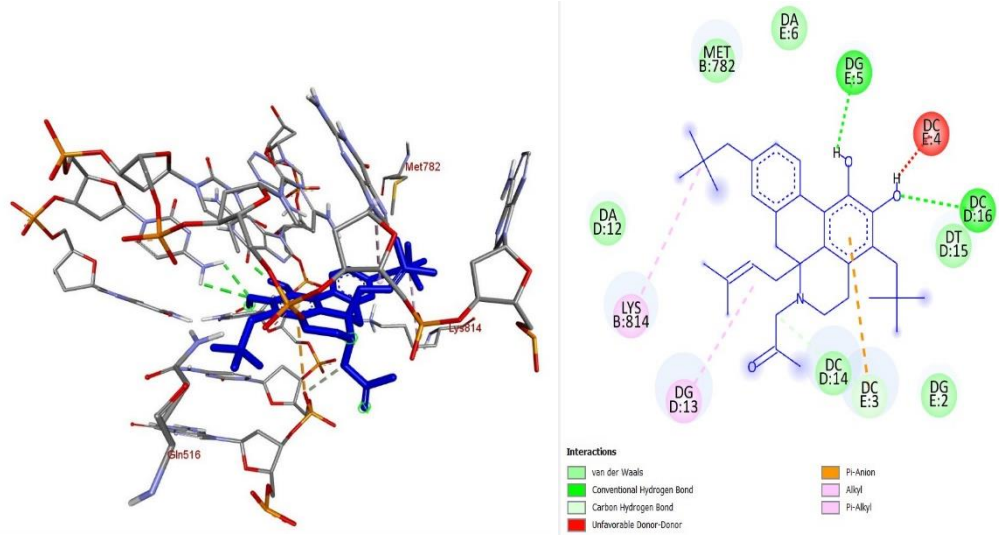

Figure 23: The 2D and 3D binding interactions of lindcarpine derivatives **(32)** against human topoisomerase II*β* (PDB ID: 3QX3).

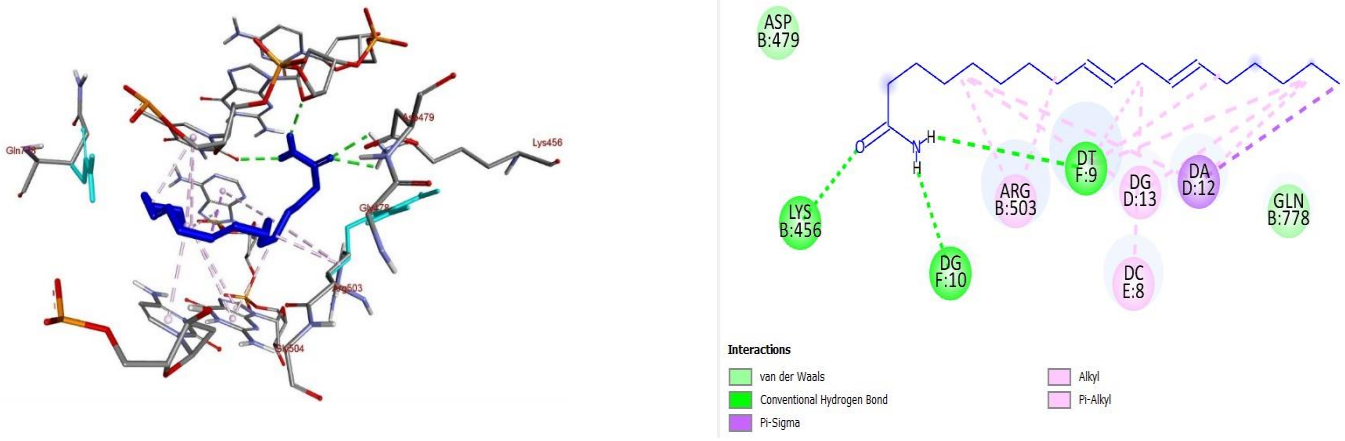

Figure 24: The 2D and 3D binding interactions of linolieamide **(33)** against human topoisomerase II*β* (PDB ID: 3QX3).

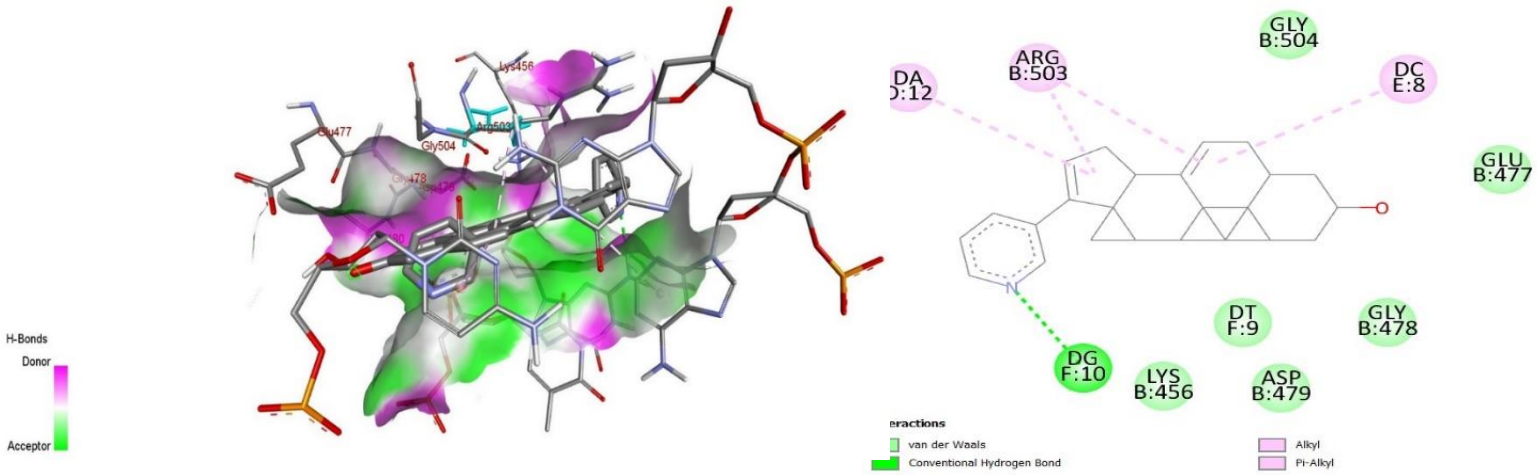

Figure 25: The 2D and 3D binding interactions of reference drug Abiraterone against human topoisomerase II*β* (PDB ID: 3QX3).

4.7 In Silico Prediction of Drug-Likeness, and Pharmacokinetic Prediction Study

Drug-likeness is a prediction that determines whether a specific organic molecule has qualities that indicate it could be an orally active drug. The isolated compounds' drug-likeness was assessed using "Lipinski's rule of five," which specifies that prospective molecules should have (MW≤500, ilog P≤5, H-bond donors ≤5, and H-bond acceptors ≤10) and Veber's parameters (TPSA ≤140 Å2 and rotatable bonds≤10**.** Linolieamide (**33**) followed Lipinski's rule of five, indicating that they are drug-like and orally active (**Table 16**). The ilog P values for all compounds are less than five except for 11-hentriacontene (**30**) and 5, 12-henicosadiene (**31**).

Table 16: Drug-likeness predictions of compounds, computed by SwissADME

Compounds	Mol. Wt. (g/mol)	NHD	NHA	NRB	TPSA ($A^{°2}$)	Log *P* (iLOGP) Lipophilicity	Log *P* (MLOGP) Lipophilicity	Log *S* (ESOL) Water Solubility	Lipinski's rule of five with zero violations
β-sitosterol (**29)**	414.71	1	1	6	20.23	4.79	6.73	− 7.90	1
11-hentriacontene (**30**)	434.82	0	0	27	0.00	8.07	9.49	− 10.88	1

5, 12-henicosadiene (**31**)	292.54	0	0	16	0.00	5.68	6.44	− 6.88	1
lindcarpine derivatives (**32**)	517.74	2	4	8	60.77	4.22	4.93	− 7.97	2
linolieamide (**33**)	279.46	1	1	14	43.09	4.00	4.06	− 4.64	0
Abiraterone	349.51	1	2	1	33.12	3.42	4.42	− 5.03	1
Amoxicillin	365.40	4	6	5	158.26	0.95	0.23	– 0.70	0

NHD = number of hydrogen donors, NHA = number of hydrogen acceptors, NRB = number of rotatable bonds, and TPSA = total polar surface area.

The ability of molecules to penetrate the outer layer of the skin is described by skin permeability (Kp). The isolated compounds' log Kp values (**Table 17**) were all determined to be within the permissible range of -1.18 to − 3.58. The SwissADME prediction parameters have shown that the GIA exhibits good oral absorption except for linolieamide (**33**). The results of the BBB permeability test performed on tested compounds (**Table 17**) demonstrated that all compounds except linolieamide (**33**) has lack of BBB permeability. In this study, 5, 12-henicosadiene (**31**) inhibited CYP1A2 inhibitor, lindcarpine derivatives (**32**) CYP2D6 inhibitor, and linolieamide (**33**) inhibited CYP1A2 inhibitor and CYP2C9 inhibitor as shown in the **Table17** below. Furthermore, glycoprotein inhibition measurements were used to predict target compound excretion properties. P-gp and cytochrome $P4_{50}$ are known to help protect biofilms (gastrointestinal tract or brain) from exogenous substance efflux (biotransformation) to protect tissues. All of the compounds except 11-hentriacontene (**30**), and lindcarpine derivatives (**32**) exhibited no inhibition of P-gp, so no liver dysfunction effects are expected after administration.

Table 17: ADME predictions of compounds, computed by SwissADME and PreADMET

Compound	Skin Permeation Value (Log *Kp*) cm/s	GI Absorption	BBB Permeability	Inhibitor Interaction					
				Pgp substrate	CYP1A2 inhibitor	CYP2C19 inhibitor	CYP2C9 inhibitor	CYP2D6 inhibitor	CYP3A4 inhibitor

β-sitosterol (**29)**	− 2.20	Low	No	No	No	No	No	No	No
11-hentriacontene (**30**)	2.46	Low	No	Yes	No	No	No	No	No
5, 12-henicosadiene (**31**)	− 1.18	Low	No	No	Yes	No	No	No	No
lindcarpine derivatives (**32**)	− 3.58	Low	No	Yes	No	No	No	Yes	No
linolieamide (**33**)	− 3.51	High	Yes	No	Yes	No	Yes	No	No
Abiraterone	− 5.14	High	Yes	No	Yes	No	No	No	No
Amoxicillin	– 9.94	Low	No	No	No	No	No	No	No

GI = gastrointestinal, BBB = blood brain barrier, P-gp = P-glycoprotein, and CYP = cytochrome-P

Table 18: Toxicity prediction of compounds, computed by ProTox-II and OSIRIS property explorer.

Compound	LD_{50} (mg/kg)	Toxicity Class	Organ Toxicity					
			Hepatotoxicity	Carcinogenicity	Immunotoxicity	Mutagenicity	Cytotoxicity	Irritant
β-sitosterol (**29)**	890	4	Inactive	Inactive	Active	Inactive	Inactive	No
11-hentriacontene (**30**)	2760	5	Inactive	Inactive	Inactive	Inactive	Inactive	No
5, 12-henicosadiene (**31**)	2760	5	Inactive	Inactive	Inactive	Inactive	Inactive	No
lindcarpine derivatives (**32**)	240	3	Inactive	Mild active	Inactive	Inactive	Inactive	No
linolieamide (**33**)	750	4	Inactive	Inactive	Inactive	Inactive	Inactive	No
Abiraterone	830	4	Inactive	Inactive	Active	Inactive	Inactive	No
Amoxicillin	15000	6	Inactive	Inactive	Inactive	Inactive	Inactive	No

5. CONCLUSION AND RECOMMENDATION

5.1 Conclusion

Natural products represent an important source of new lead compounds in drug discovery research. *S. multiflorus* is one of the medicinal plants used traditionally to heal various infectious diseases. The root of the plant (400 g) was extracted with n-hexane, chloroform, and methanol solvents successively to afford 1, 1.125, and 12.25% yields respectively. Chromatographic separation of the crude extracts of hexane and chloroform furnished *β*-sitosterol (**29**), 11-hentriacontene (**30**), 5, 12-henicosadiene (**31**), lindcarpin derivatives (**32**)**,** and linoliamide (**33**). The extracts and isolated compounds were also evaluated *in vitro* for antibacterial activities using the disc diffusion method among them *β*-sitosterol (**29)** *(15±0.00mm) and* 5, 12-henicosadiene (**31**) *(15±0.00mm) showed promising activity against S. typhimurium compared to ciprofloxacin (31.3±1.97).* Linoliamide (**33**) and *β*-sitosterol (**29)** had slightly highest scavenging of DPPH free radicals than other isolated compounds but less activity when compared to ascorbic acid. *In silico* molecular docking analysis was done using Autodock and it was found that among isolated compounds *β*-sitosterol (**29**) exhibited better docking efficiency with (*E.coli*) enzyme DNA gyrase displaying a binding affinity of −9.1 kcal/mol more than amoxicilin (–7.6 kcal/mol) and *β*-sitosterol (**29)** also exhibited better docking efficiency against human topoisomerase II*β* enzymes with binding affinity of 9.6 kcal/mol compared with standard Abiraterone (-11.8 kcal/mol), and also lindcarpine derivatives (**32**) (−7.3 kcal/mol) exhibited better docking efficiency against *S. aureus* Pyruvate Kinase. This suggests that compound *β*-sitosterol (**29)** and lindcarpine derivatives (**32**) may be used as potential drug lead candidates.

5.2 Recommendation

Further biological activity (antifungal, anticancer, and cytotoxicity) on crude extracts as well as isolated compounds are required to validate the traditional use of the plant. Additionally, 2D NMR spectroscopic techniques (HMBC, HSQC, COSY, and NOESY) and MS studies are required to have a better understanding of structural and chemical parameters required to develop related drug lead compounds. Further study is recommended on other parts of the plant such as the seed, leaf, and bark.

REFERENCE

Abate, L., Tadesse, M. G., Bachheti, A., & Bachheti, R. K. (2022). Review Article Traditional and Phytochemical Bases of Herbs, Shrubs, Climbers, and Trees from Ethiopia for Their Anticancer Response. *Biomed Research International*, *2022*, 1–27.

Abdallah, O. M., Ali, A. A., & Itokawa, H. (1989). An alkaloid from *Haemanthus*. *Phytochemistry*, *28*(11), 3248 3249.

Adewusi, E. A., & Steenkamp, V. (2011). In vitro screening for acetylcholinesterase inhibition and antioxidant activity of medicinal plants from southern Africa. *Asian Pacific Journal of Tropical Medicine*, *4*(10), 829–835. https://doi.org/10.1016/S1995-7645(11)60203-4

AFROZ, S. (2018). *Taxonomy and Reproductive Biology of the Family Liliaceae of Bangladesh.* (Issue 102).

Akhlas, M. B., Chowdhury, Md. Mashrur Hossain, R., Parvin, T., Khatun, F., Akter, A., Muhammad, T. I., & Razina, R. (2021). Phyto-Pharmacological Investigation of Aqueous Crude Extract Phyto-Pharmacological Investigation of Aqueous of *Scadoxus Multiflorus*. *World Journal of Pharmacy and Pharmaceutical Sciences*, *10*(10), 154–173. https://doi.org/10.20959/wjpps202110-20286

Ali, A., Sayed, H., Abdalla, O., Steglich, W., & Dagne, E. (1987). Alkaloids From *Haemanthus multiflorus* Martyn. *Bull. Pharm. Sci*, *10*(1), 157–164.

Aliba, M. O., Ndukwe, I. G., & Ibrahim, H. (2018). Isolation and characterization of *β*-sitosterol from methanol extracts of the stem bark of large-leaved rock fig (*Ficus abutilifolia* Miq). *Journal of Applied Sciences and Environmental Management*, *22*(10),

1639. https://doi.org/10.4314/jasem.v22i10.19

Anza, M., Endale, M., Cardona, L., Cortes, D., Eswaramoorthy, R., Zueco, J., Rico, H., Trelis, M., & Abarca, B. (2021). Antimicrobial activity, in silico molecular docking, ADMET, and DFT analysis of secondary metabolites from roots of three Ethiopian medicinal plants. *Advances and Applications in Bioinformatics and Chemistry*, *14*, 117–132. https://doi.org/10.2147/AABC.S323657

Ateş, H., & Yalçin, E. (2022). Therapeutic Source: Plants. *Black Sea Journal of Agriculture*, 336–343. https://doi.org/10.47115/bsagriculture.1078368

Babu, S., & Jayaraman, S. (2020). An update on *β*-sitosterol: A potential herbal nutraceutical for diabetic management. *Biomedicine and Pharmacotherapy*, *131*, 110702. https://doi.org/10.1016/j.biopha.2020.110702

Bargah, & Rohit. (2015). The preliminary test of phytochemical screening of crude ethanolic and aqueous extract of *Moringa pterygosperma* Gaertn. *Journal of Pharmacognosy and Phytochemistry*, *4*(1), 7–9.

Bødker, K. H. (2020). *Fireball lilies of Africa: a molecular phylogeny of the genus Scadoxus Raf. (Amaryllidaceae).*

Brand-Williams, W., Cuvelier, M. E., & Berset, C. (1995). Use of a free radical method to evaluate antioxidant activity. *LWT - Food Science and Technology*, *28*(1), 25–30. https://doi.org/10.1016/S0023-6438(95)80008-5

Cahlíková, L., Benešvá, N., Macáková, K., Urbanová, K., & Opletal, L. (2011). GC/MS analysis of three Amaryllidaceae species and their cholinesterase activity. *Natural Product Communications*, *6*(9), 1255–1258.

https://doi.org/10.1177/1934578x1100600912

Calixto, J. B. (2019). The role of natural products in modern drug discovery. *Anais Da Academia Brasileira de Ciencias*, *91*, 1–7. https://doi.org/10.1590/0001-3765201920190105

Chhabra, S. C., Mahunnah, B. L. A., & Mshiu, E. N. (1987). Plants used in traditional medicine in eastern Tanzania. I. Pteridophytes and angiosperms (Acanthaceae to canellaceae). *Journal of Ethnopharmacology*, *21*(3), 253–277. https://doi.org/10.1016/0378-8741(87)90103-6

Das, R., Goswami, S., Barman, A., Barman, M., & Ray, S. (2021). Antimitotic and cytotoxic effects of leaf aqueous extract of scadoxus multiflorus (Martyn) Raf. In allium cepa root apical meristem cells. *Cytologia*, *86*(3), 267–271. https://doi.org/10.1508/cytologia.86.267

Demissew, S., & Nordal, I. (2010). *Aloes and Lilies of Ethiopia and Eritrea*.

Emam, A. J., Yaya, E. E., Choudhary, I. M., Yousuf, S., & Gebremedhin, M. T. (2022). In Vitro Anticancer Activities of Selected Ethiopian Plant Extracts on HeLa and Lines, P C Cell. *Ethiopian Pharmaceutical Journal*, *37*, 77–82. https://doi.org/10.4314/epj.v37i1.6

Fadlan, A., & Nusantoro, Y. R. (2021). The Effect of Energy Minimization on The Molecular Docking of Acetone-Based Oxindole Derivatives. *JKPK (Jurnal Kimia Dan Pendidikan Kimia)*, *6*(1), 69. https://doi.org/10.20961/jkpk.v6i1.45467

Fishchuk, O., & Odintsova, A. (2021). Micromorphology and Anatomy of the Flowers in Clivia spp . and Scadoxus multiflorus (Haemantheae, Amaryllidaceae). *Acta Agrobotanica*, *74*, 1–17. https://doi.org/10.5586/aa.7417

Francesc, V., Bastida, J., & Nair, J. J. (1997). Alkaloids of the South African Amaryllidaceae : A Review. *Recent Res. Devel. in Phytochemical*, *1*, 132–171.

Gashu, M. (2018). *Antifungal Natural Products against two Plant Diseases : Root rot/wilt of Faba Bean and Late Blight of Potato*.

Hanh, T. T. H., Hang, D. T. T., Van Minh, C., & Dat, N. T. (2011). Anti-inflammatory effects of fatty acids isolated from Chromolaena odorata. *Asian Pacific Journal of Tropical Medicine*, *4*(10), 760–763. https://doi.org/10.1016/S1995-7645(11)60189-2

Kamal, T., Muzammil, A., Akintunde, R., Rahma, M., & Omar, M. (2012). Preliminary phytochemical screening test of Garcinia griffithii Plant. *Innova Cienta*, *4*(4l).

Koutova, D., Maafi, N., Havelek, R., Blunden, G., Rez, M., & Cahl, L. (2020). Chemical and Biological Aspects of Montanine-Type Alkaloids Isolated from Plants of the Amaryllidaceae Family. *Molecules*, *25*(2337), 1–19.

Kumar. (2010). Crystal structure determination and inhibition studies of novel xylanase and -amylase. *FEBS Journal*, *277*, 2868–2882.

Kwembeya, E. G. (2021). Tracking biological footprints of climate change using flowering phenology of the geophytes : Pancratium tenuifolium and Scadoxus multiflorus. *International Journal of Biometeorology*, *65*, 577–586.

Mansourian, M., Fassihi, A., Saghaie, L., Madadkar-Sobhani, A., Mahnam, K., & Abbasi, M. (2015). QSAR and docking analysis of A2B adenosine receptor antagonists based on the non-xanthine scaffold. *Medicinal Chemistry Research*, *24*(1), 394–407. https://doi.org/10.1007/s00044-014-1133-7

Mariita, R. M., Ogol, C. K. P. O., Oguge, N. O., & Okemo, P. O. (2011). Methanol extract from three medicinal plants from Samburu in Northern Kenya shows significant antimycobacterial, antibacterial, and antifungal properties. *Research Journal of Medicinal Plant*, *5*(1), 54-64.

Meerow, A. W., & Snijman, D. A. (1998). Amaryllidaceae. *Flowering Plants · Monocotyledons*, 83–110. https://doi.org/10.1007/978-3-662-03533-7_11

Mir, M. A., Parihar, K., Tabasum, U., & Kumari, E. (2016a). *4-5-10-775.Pdf*. *4*(5), 171–174.

Mir, M. A., Parihar, K., Tabasum, U., & Kumari, E. (2016b). Estimation of alkaloid, saponin, and flavonoid, content in various extracts of Crocus sativa. *Journal of Medicinal Plant Studies*, *4*(5), 171–174.

Monkheang, P., Chaveerach, A., Sudmoon, R., & Tanee, T. (2016). Karyotypic features include organizations of the 5s, 45S rDNA loci, and telomeres of Scadoxus multiflorus (Amaryllidaceae). *Comparative Cytogenetics*, *10*(4), 637–646. https://doi.org/10.3897/CompCytogen.v10i4.9958

Mwamidi, D. M., Mwasi, S. M., & Nunow, A. A. (2012). Indigenous Knowledge of Taita Community in the Use and. *J.Bio.Innov1*, *8330*(4), 77–86.

Naidoo, D. (2016). *In vitro propagation, phytochemistry, and pharmacology of the blood lily, Scadoxus puniceus*.

Naidoo, D., Gruz, J., Po, L., Finnie, J. F., Biba, O., Dole, K., & Staden, J. Van. (2017). Metabolite profiling and isolation of biologically active compounds from Scadoxus puniceus, a highly traded South African medicinal plant. *Phytotherapy Research*, 1–6. https://doi.org/10.1002/ptr.6000

Najmi, A., Javed, S. A., Al Bratty, M., & Alhazmi, H. A. (2022). Modern Approaches in the Discovery and Development of Plant-Based Natural Products and Their Analogues as Potential Therapeutic Agents. *Molecules*, *27*(2). https://doi.org/10.3390/molecules27020349

Nwodo, O., & Nkwocha, P. (2015). Qualitative and Quantitative Phytochemical Screening of the Aqueous Leaf Extract of Senna mimosoides : Its Effect in vivo Leukocyte mobilization induced by the inflammatory stimulus. *International Journal of Current Microbiology and Applied Science*, *4*(5), 1176–1188.

Pagning, A. L. N., Tamokou, J., Khan, M. L., Ali, M. I., Hameed, A., Ngnokam, D., Tapondjou, L. A., Kuiate, J., & Ali, M. S. (2016). South African Journal of Botany Antimicrobial, antioxidant and butyrylcholinesterase inhibition activities of extracts and isolated compounds from Scadoxus pseudocaulus and semi-synthetic farrerol derivatives. *South African Journal of Botany*, *102*, 166–174. https://doi.org/10.1016/j.sajb.2015.06.009

Praiwala, B., Priyanka, S., Raghu, N., Gopenath, N., Gnanasekaran, A., Karthikeyan, M., Indumathi, R., Ebrahim, N. K., Pugazhandhi, B., Pradeep, P., Ranjith, M. S., Balasubramanian, S., & Basalingappa, K. M. (2019). In vitro antibacterial activity of Tinospora cordifolia leaf extract and its phytochemical screening. *Journal of Biomedical Sciences*, *5*(2), 10–17. https://doi.org/10.3126/jbs.v5i2.23633

Rani, P., & Khullar, N. (2004). Antimicrobial evaluation of some medicinal plants for their anti-enteric potential against multi-drug resistant Salmonella typhi. *Phytotherapy Research*, *18*(8), 670–673. https://doi.org/10.1002/ptr.1522

Santhi, K., & Sengottuvel, R. (2016). Qualitative and Quantitative Phytochemical analysis of

Moringa concanensis Nimmo. *International Journal of Current Microbiology and Applied Sciences*, *5*(1), 633–640. https://doi.org/10.20546/ijcmas.2016.501.064

Seoposengwe, K., van Tonder, J. J., & Steenkamp, V. (2013). In vitro neuroprotective potential of four medicinal plants against rotenone-induced toxicity in SH-SY5Y neuroblastoma cells. *BMC Complementary and Alternative Medicine*, *13*, 1–11. https://doi.org/10.1186/1472-6882-13-353

Simpson, M. G. (2010). Diversity and Classification of Flowering Plants. In *Plant Systematics* (Vol. 229). https://doi.org/10.1016/b978-0-12-374380-0.50007-5

Son, H. D., Yun, S. A., Kim, S. C., & Im, H. T. (2020). Hydrocarbon patterns in cleisostoma scolopendrifolium (Orchidaceae) as a key mechanism for pollination. *Korean Journal of Plant Taxonomy*, *50*(2), 148–153. https://doi.org/10.11110/kjpt.2020.50.2.148

Tadesse, A., Tsegay, B. A., & Telake, B. B. (2018). Ethnoveterinary medicinal plants in rural settings of Bahir. *Ethiop J Sci Technol.*, *11*(3), 223–251.

Tagliabue, A., & Rappuoli, R. (2018). Changing priorities in vaccinology: Antibiotic resistance moving to the top. *Frontiers in Immunology*, *9*(MAY), 1–9. https://doi.org/10.3389/fimmu.2018.01068

Truong, D. H., Nguyen, D. H., Ta, N. T. A., Bui, A. V., Do, T. H., & Nguyen, H. C. (2019). Evaluation of the use of different solvents for phytochemical constituents, antioxidants, and in vitro anti-inflammatory activities of severinia buxifolia. *Journal of Food Quality*. https://doi.org/10.1155/2019/8178294

Tuasha, N., Petros, B., & Asfaw, Z. (2018). Plants Used as Anticancer Agents in the Ethiopian Traditional Medical Practices: A Systematic Review. *Evidence-Based*

Complementary and Alternative Medicine, *2018*, 1–29. https://doi.org/10.1155/2018/6274021

Veeresham, C. (2012). Natural products derived from plants as a source of drugs. *Journal of Advanced Pharmaceutical Technology and Research*, *3*(4), 200–201. https://doi.org/10.4103/2231-4040.104709

WHO, W. H. O. (2002). *Traditional Medicine Strategy (2002–2005)*.

Yokosuka, A., Suzuki, N., & Mimaki, Y. (2017). Phytochemistry Letters Chemical constituents of the bulbs of Haemanthus multiflorus. *Phytochemistry Letters*, *21*, 6–10. https://doi.org/10.1016/j.phytol.2017.05.007

APPENDIX

Appendix 1: ^{1}H NMR spectrum of compound **29**

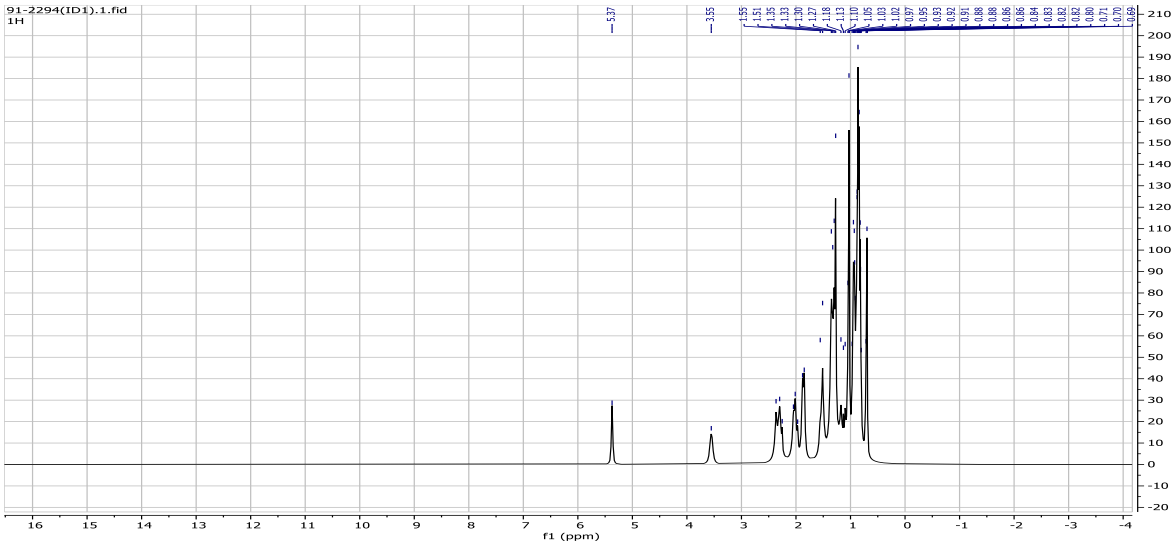

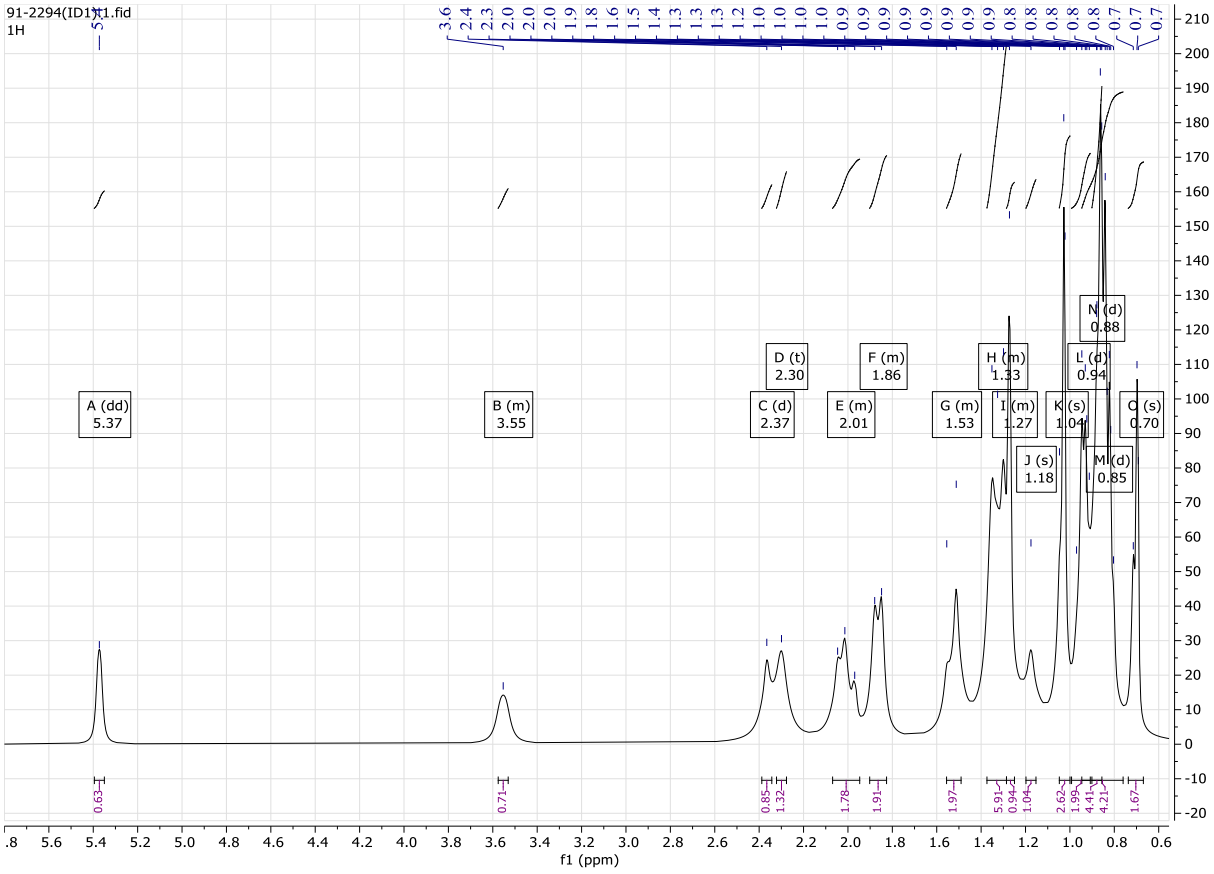

Appendix 2: ^{13}C NMR spectrum of compound **29**

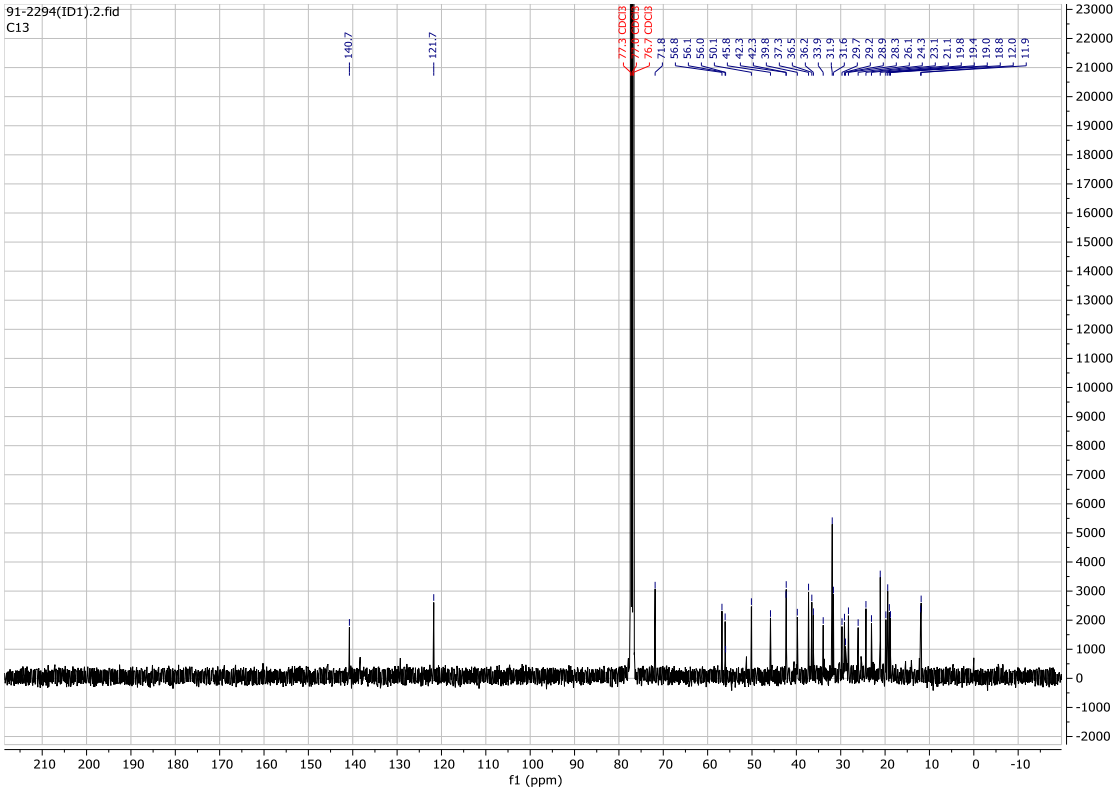

Appendix 3: DEPT-135 spectrum of compound **29**

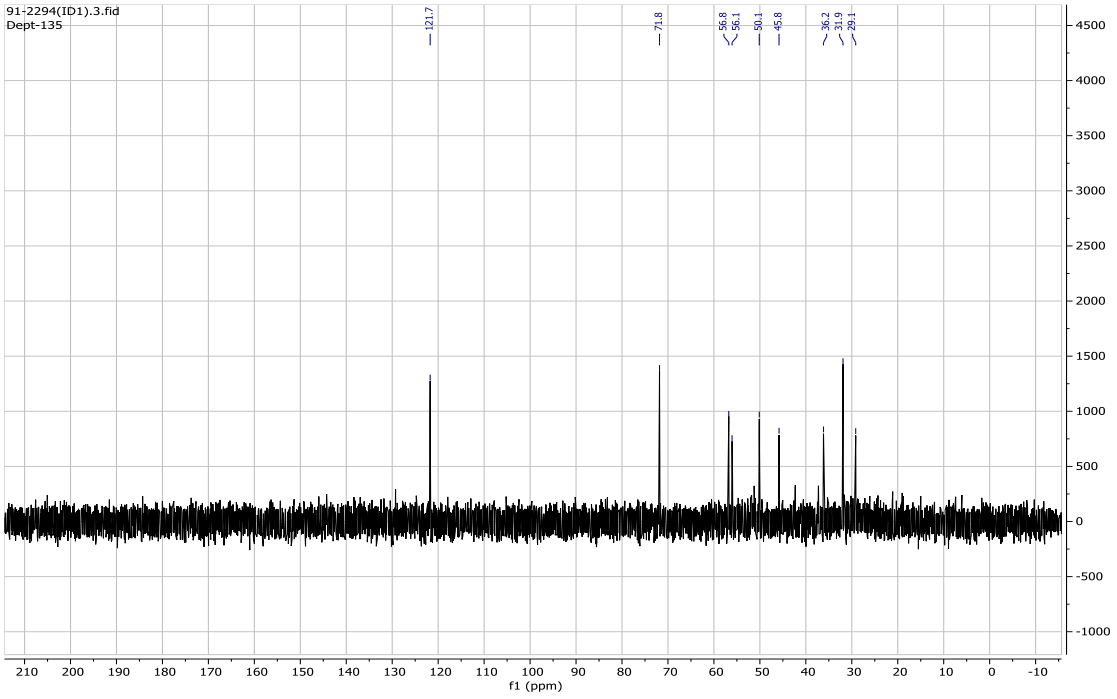

Appendix 4: ^{1}H NMR spectrum of compound **30**

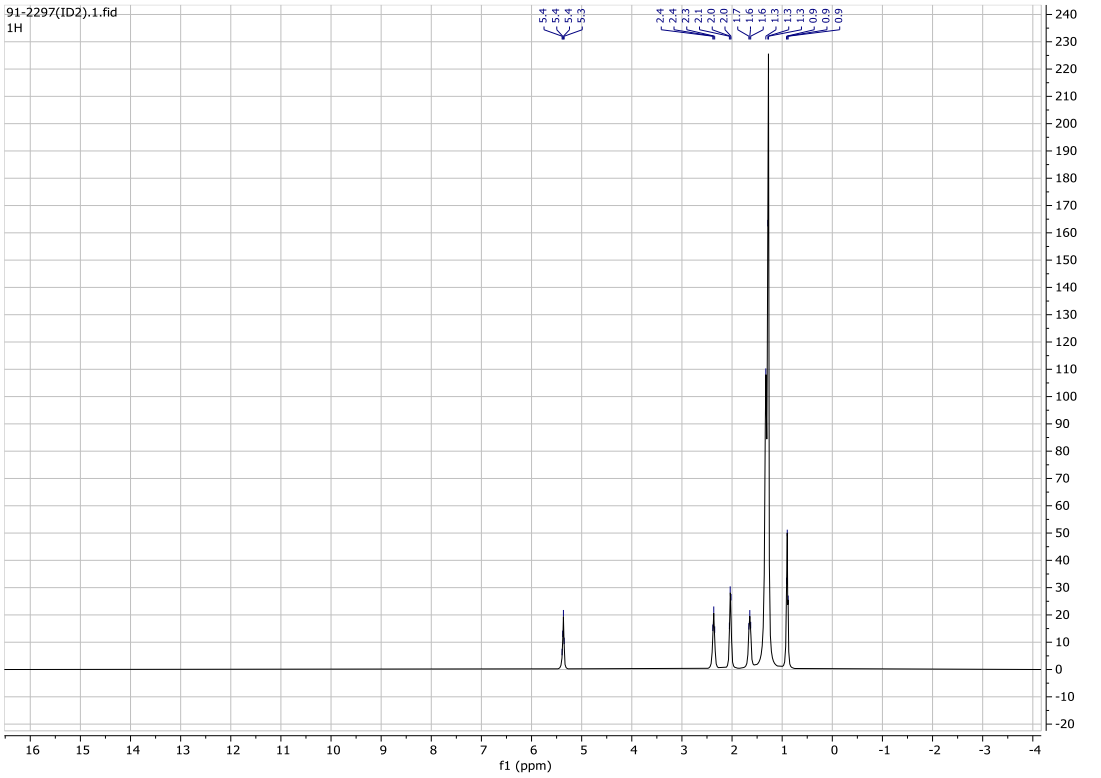

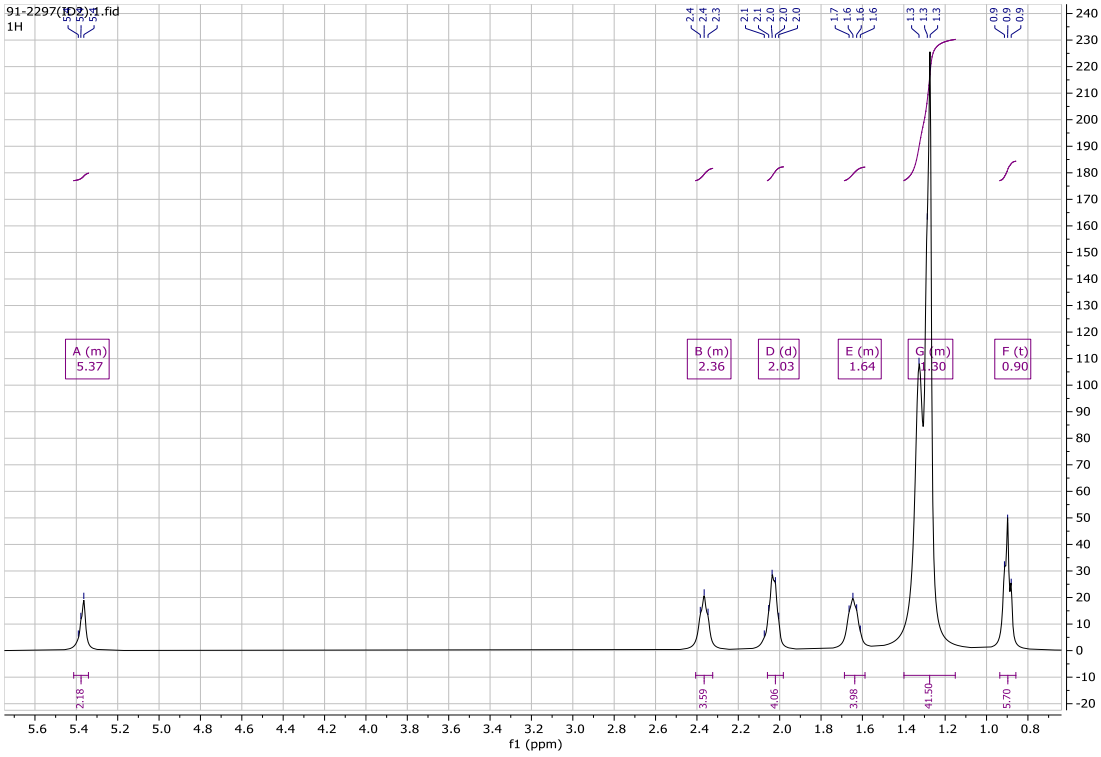

Appendix 5: ^{13}C NMR spectrum of compound **30**

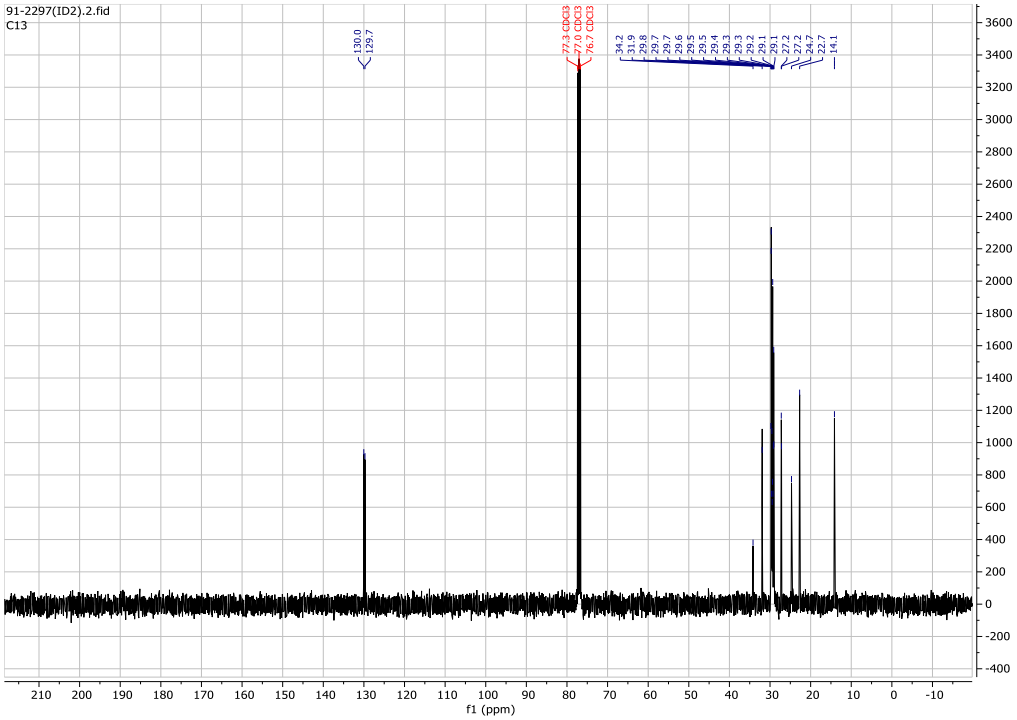

Appendix 6: DEPT-135 spectrum of compound **30**

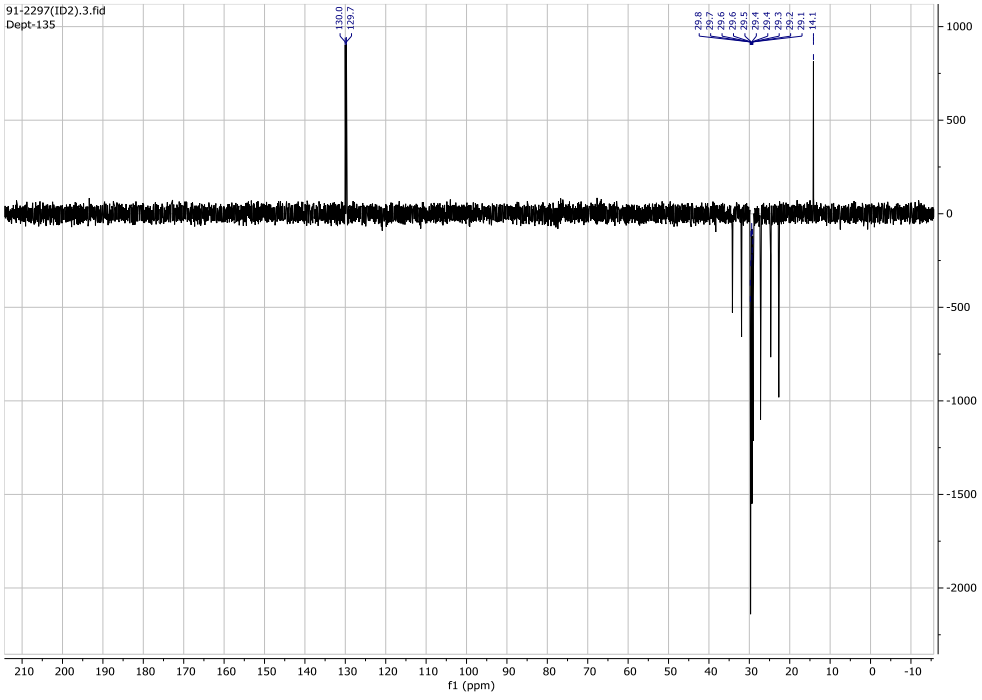

Appendix 6: ^{1}H NMR spectrum of compound **3**1

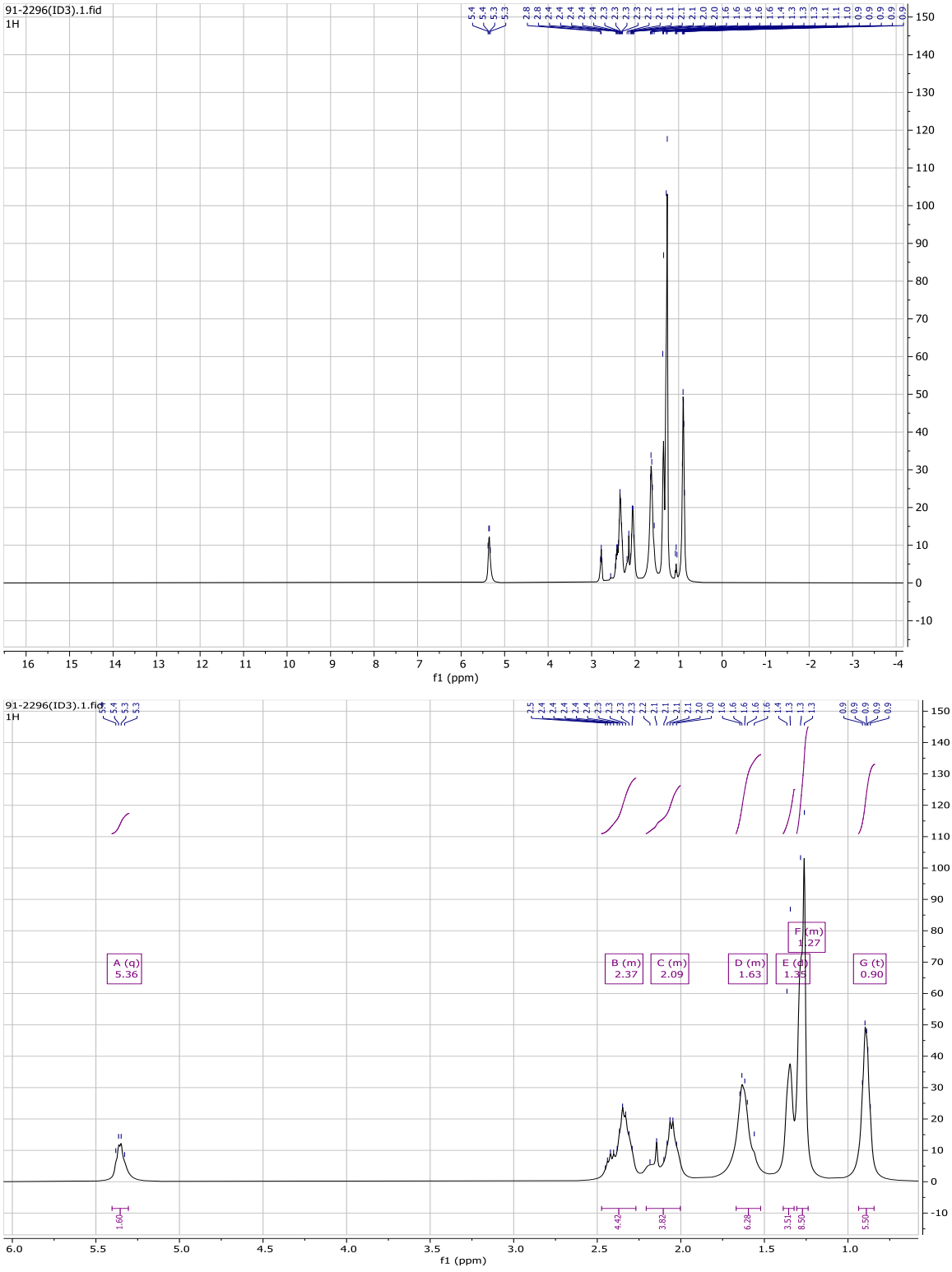

Appendix 7: ^{13}C NMR spectrum of compound **31**

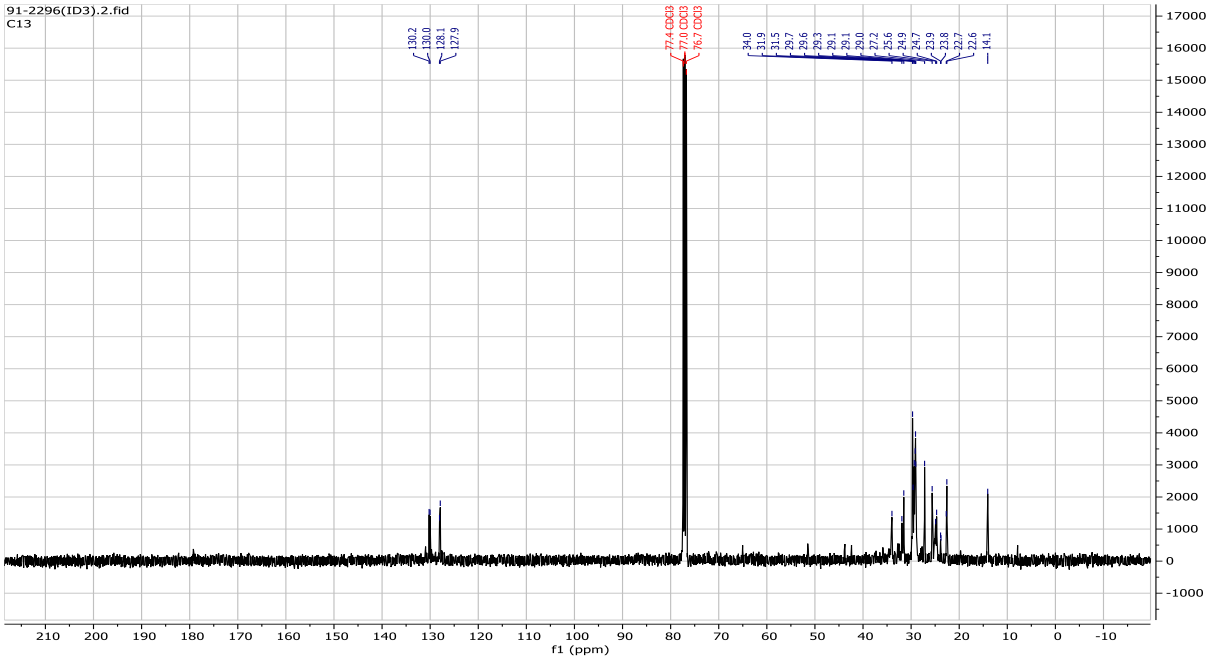

Appendix 8**: DEPT-135 NMR spectrum of compound** 31

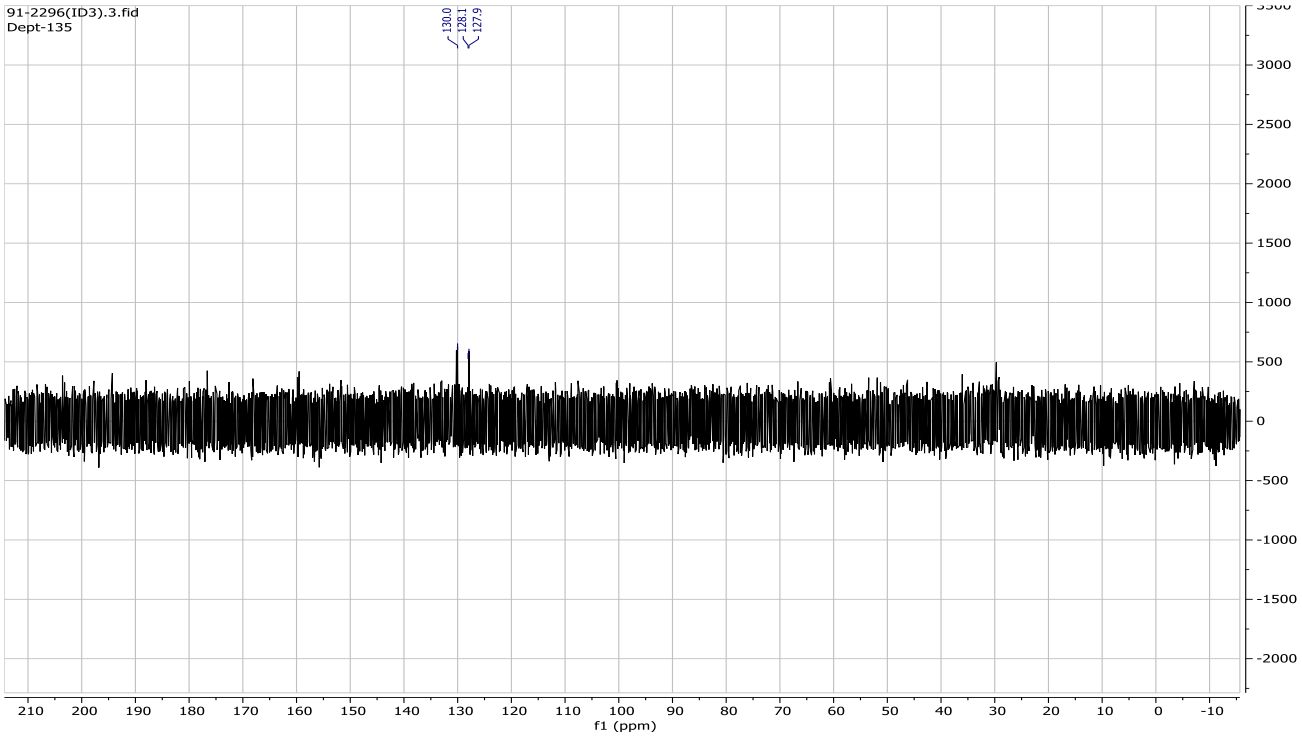

Appendix 9: ^{1}H NMR spectrum of compound **32**

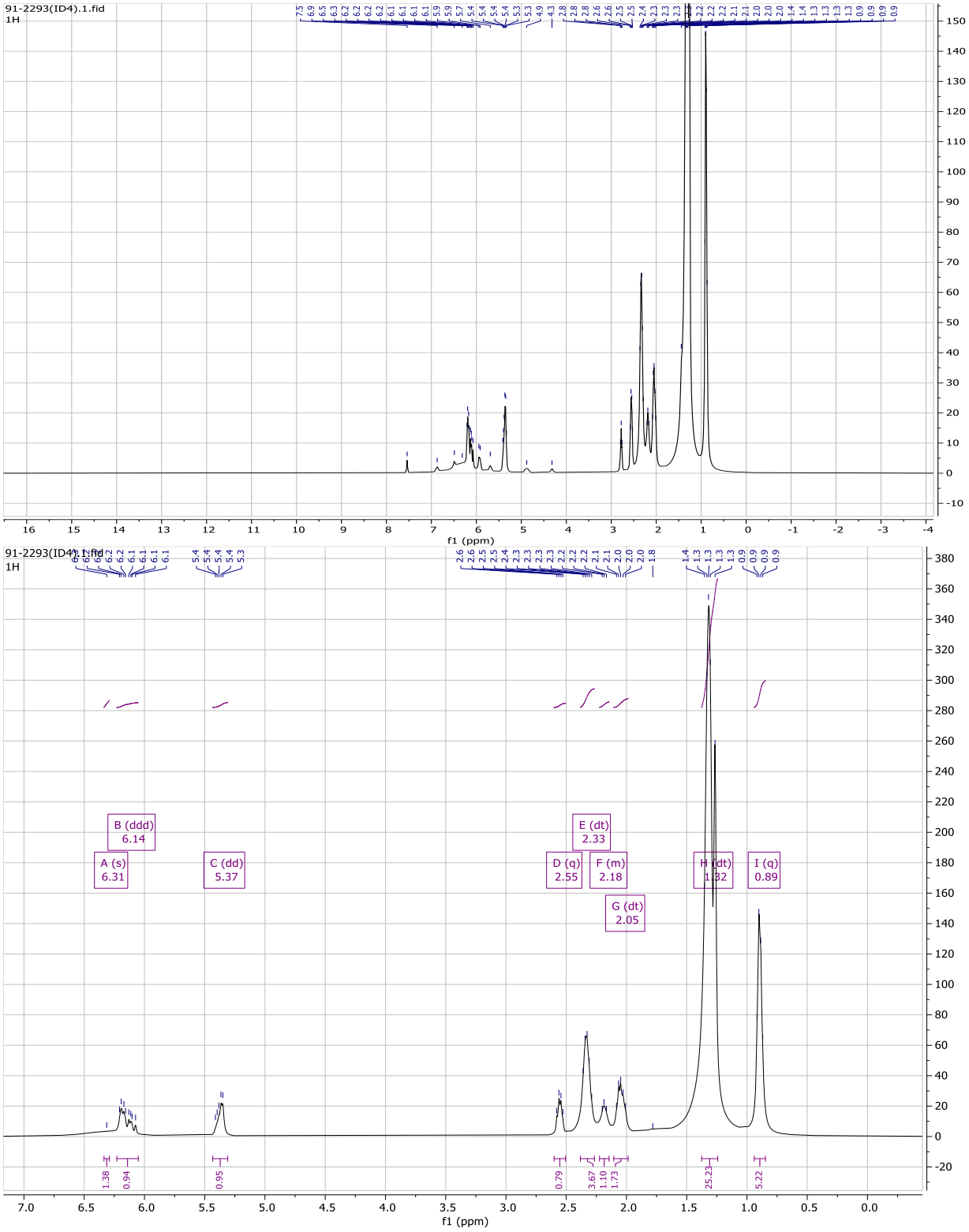

Appendix 10: ^{13}C NMR spectrum of compound **32**

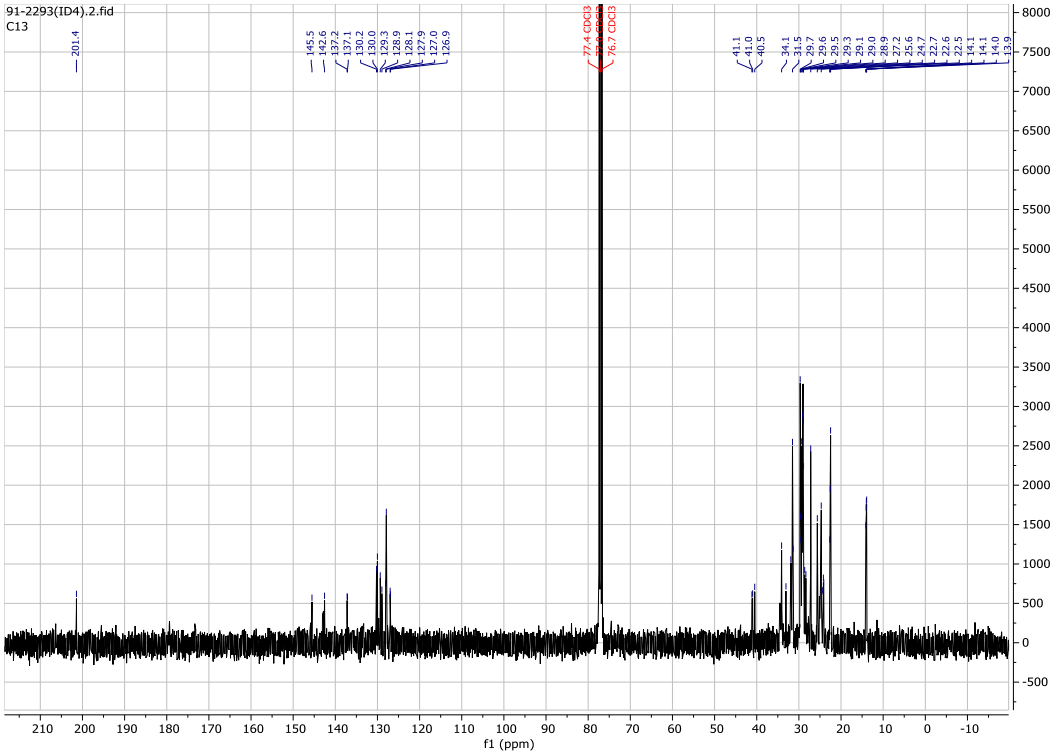

Appendix 11: DEPT-135 spectrum of compound **32**

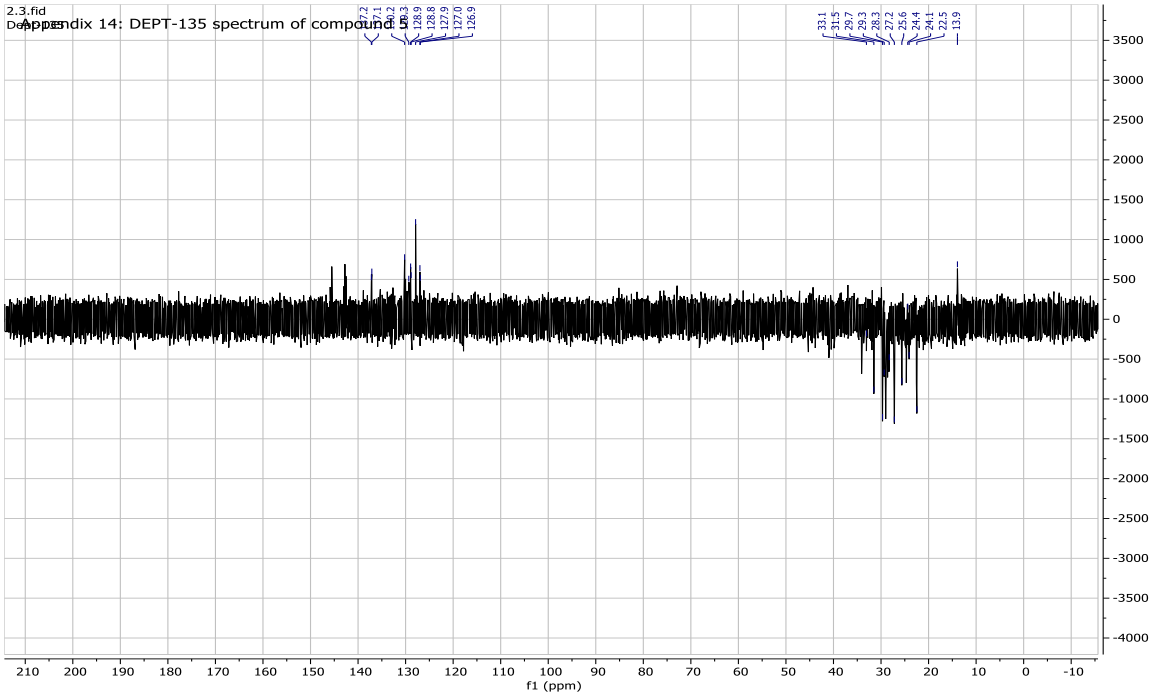

Appendix 12: ^{1}H NMR spectrum of compound **33**

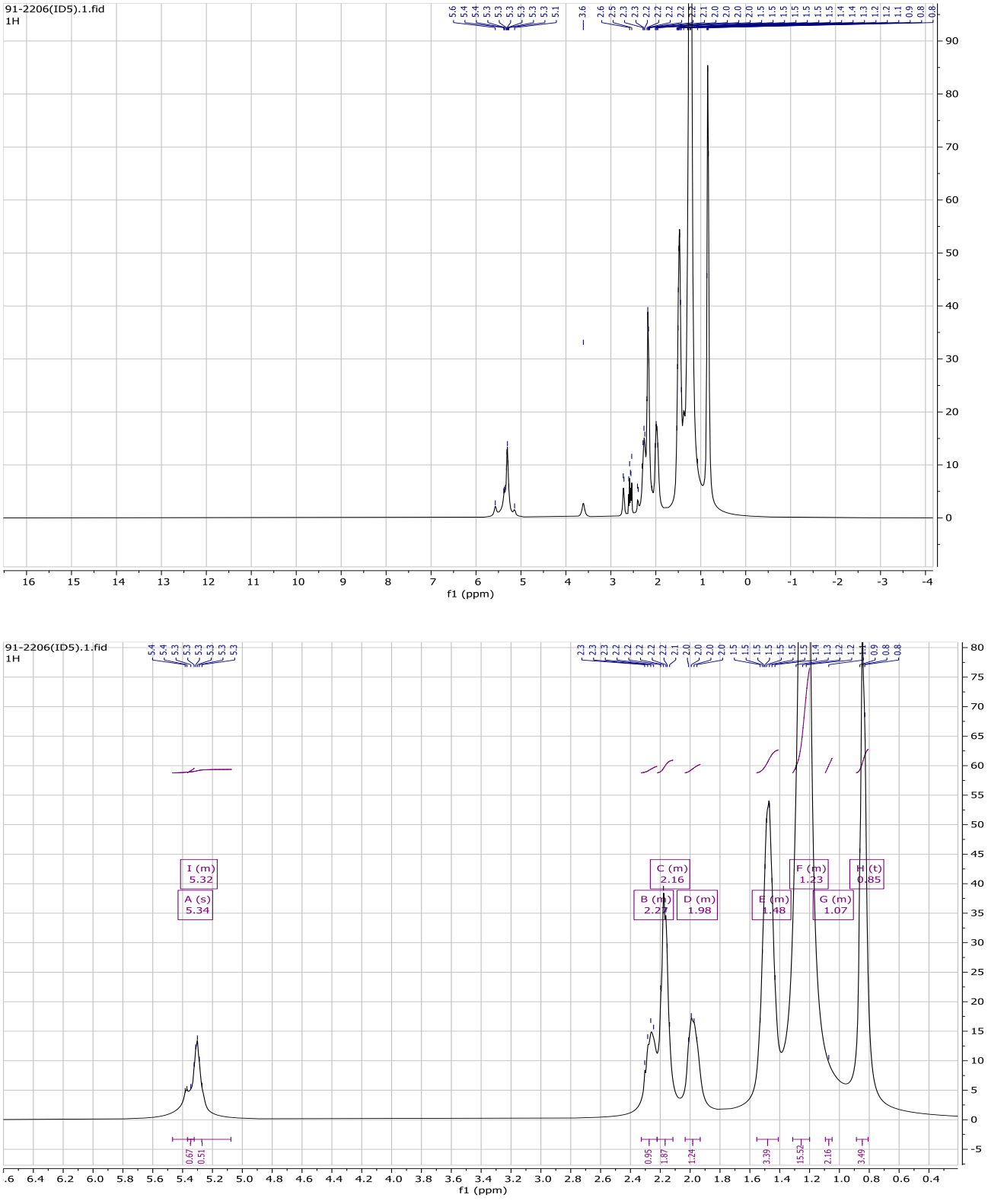

Appendix 13: ^{13}C NMR spectrum of compound **33**

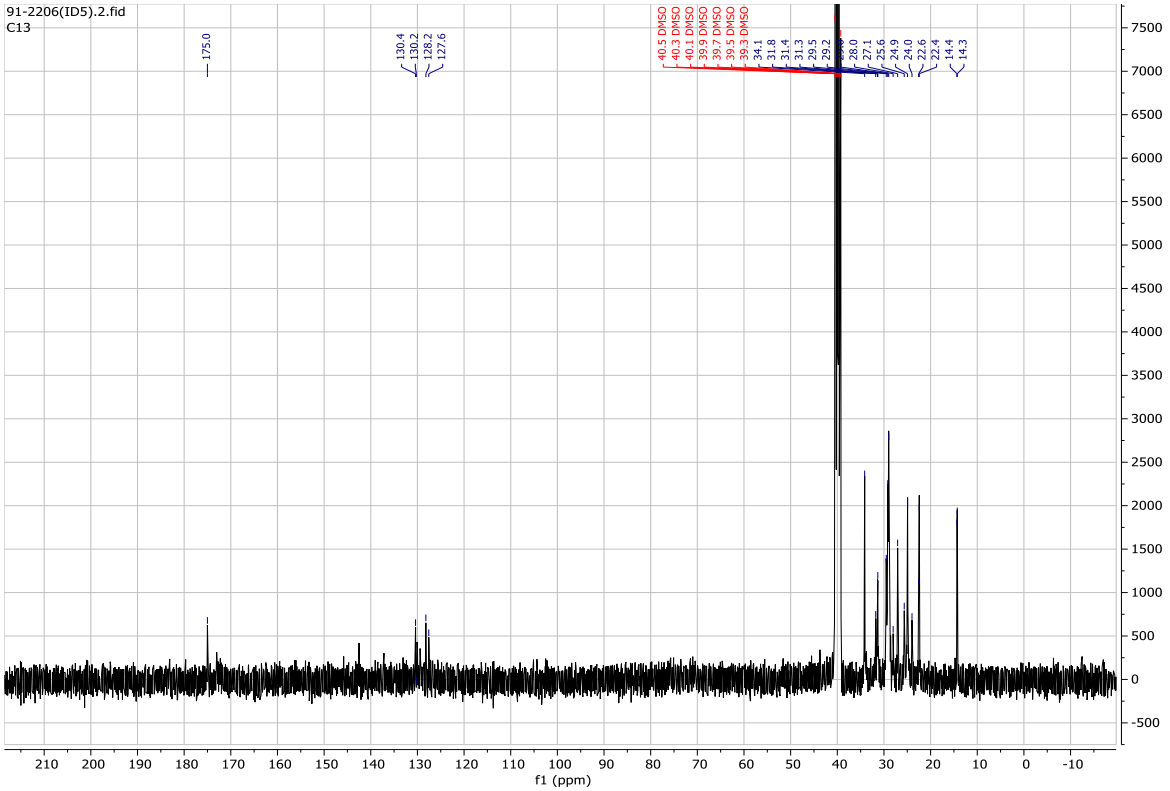

Appendix 14: DEPT-135 spectrum of compound **33**